# CIRCULAR-ARRAY RADAR ANTENNA:
## PENCIL-BEAM FORMING AND PHASING TECHNIQUES

Combination of linear and cylindrical-array beam-forming techniques is shown to be a feasible means of producing a pencil beam

J.H. Provencher and A.D. Munger

Research and Development Report

12 March 1968

## PROBLEM

Develop techniques for wide-frequency spectrum, agile-beam antennas for radar. Determine elevation-scanning limitations of cylindrical configurations, and study techniques for achieving pencil beams from such configurations.

## RESULTS

1. Several linear and ring-array beam-forming techniques were examined, as part of the investigation directed at achieving pencil-beam antennas from cylindrical configurations.

2. The SAMB (Stationary Aperture Moving Beam) and CARAMBA (Circular-Array Radar Agile Moving Beam Antenna) concepts show promise for extension to cylindrical configurations; the SAMB program yields excellent characteristics over a 25-percent frequency band and individual beam-pointing angles do not change with frequency. Low-side-lobe ring arrays are achievable by means of CARAMBA techniques.

3. Preliminary computer predictions indicate that a combination of the lens-feed technique and a linear array as an element of a ring array is a possible method of enabling a cylindrical array to produce a pencil beam. Some preliminary performance predictions are included.

## RECOMMENDATIONS

1. Investigate the implementation of a sector of a cylindrical array to produce a pencil beam.

2. Verify experimental computer predictions of optimum excitation distributions, and of elevation-scanning limitations and approximations.

3. Investigate techniques to provide multi-aperture, multifrequency capability to the cylindrical array.

## ADMINISTRATIVE INFORMATION

Work was performed under SF 001 02 05, Task 6072 (NELC D11571), by members of the Radar Division as a portion of the antenna techniques program. The report covers work from September 1967 to January 1968 and was approved for publication 12 March 1968.

The computer programs were written by R. F. Arenz of the NELC Mathematical Analysis Center. The SAMB program was conceived by B. I. Small of the Radar Division.

# CONTENTS

# ILLUSTRATIONS

# INTRODUCTION

In the continuing effort to develop shipborne radar systems capable of meeting military needs, important objectives have been broad-spectrum signals, low-side-lobe antennas, and bearing agility independent of frequency. Integration of electronic systems (as in the use of the same antenna structure for several functions and at various frequencies) has been stressed, to reduce space, weight, and manning. Previous studies have shown that the antenna of the circular-array type for a single ring of elements is both effective and feasible in meeting these objectives. A natural outcome of the wide-spectrum ring-array development was the use of a linear array as an element for a cylindrical array (fig. 1).

Reference 1 (see list at end of report) describes the preliminary feasibility investigation of the ring-array concept, presents design parameters for cylinder-backed ring and arc configurations, and establishes three areas for continuing investigation. The second, and part of the third, of the recommended study areas have been completed and are reported in references 2-4. Briefly, the work included theoretical studies and computations relating ring-array current distributions to array radiation patterns; formulation of beamwidth and amplitude and phase distribution for use in designing narrowbeam, low-side-lobe, circular-array antennas; and design and test of a 128-element ring-array antenna, using an R-2R parallel-plate lens feed system, with beam position electronically steerable in discrete steps. Another phase of the third study recommended had to do with power dividing and phasing techniques and the possibility of combining linear and circular array techniques for use in two coordinate azimuthly symmetrical arrays. The work to be reported here was performed as part of that study and, in particular, is concerned with methods of beam-forming to obtain pencil beams from a cylindrical configuration of elements.

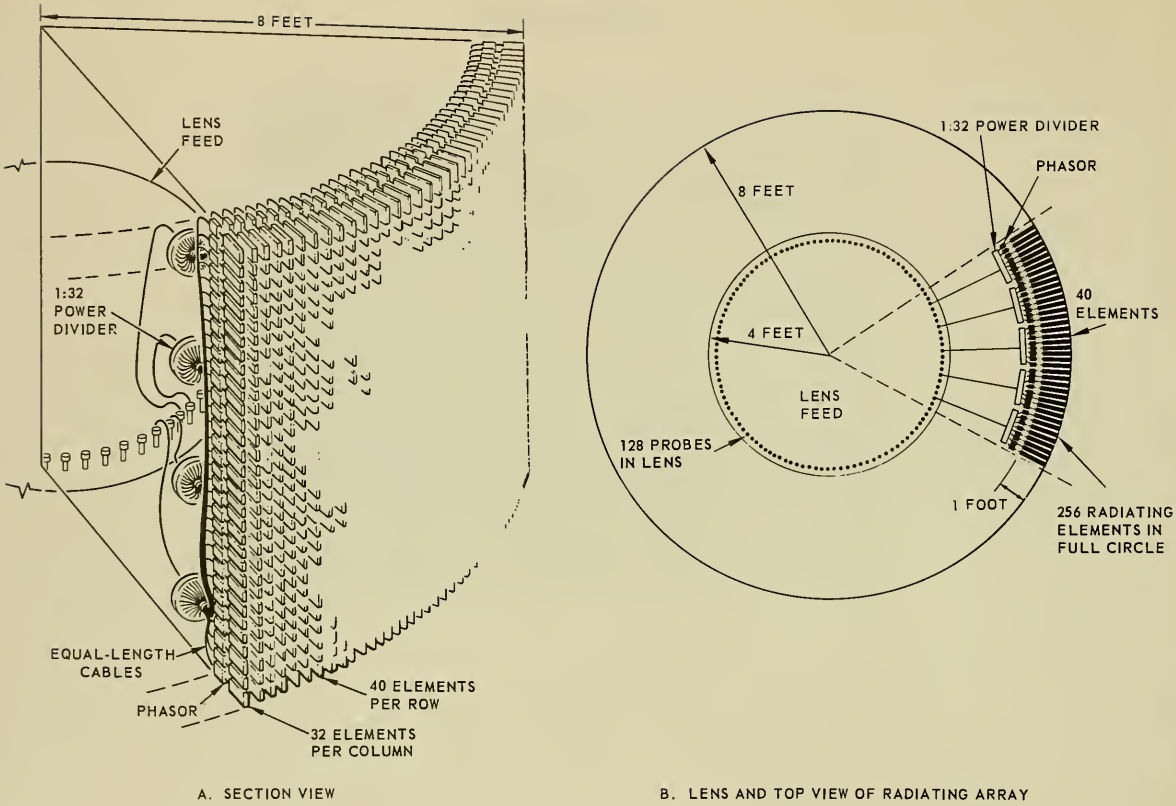


Figure 1. Sectional and top views of cylindrical array.

In initiating the investigation reported here, advances in the basic design approach (as noted briefly above) furnished valuable guidelines. Some techniques successfully implemented for linear and planar arrays were adaptable for use in a cylindrical configuration; and methods of beam-forming and steering already implemented by NELC for various IFF and radar applications were incorporated where possible.

Techniques involved in the SAMB (Stationary Aperture Moving Beam) and CARAMBA (Circular-Array Radar Agile Moving Beam Antenna) programs were important in the present study. However, they were of direct concern only as they might be extended to a pencil-beam radar antenna having a circularly symmetric configuration. Only such pertinent details are furnished here, except for some aspects of the SAMB program which have not been previously reported. The computer programs associated with the SAMB and CARAMBA antennas, and descriptions of their circuitry and switching, are not of concern here and have not been included.

## THE SAMB ANTENNA

With the advent of the fixed-aperture scanning arrays of the AN/SPS-32 and SPS-33 types, the need for a rapid-scanning, highly agile antenna for the IFF function became apparent. SAMB was part of the effort to fill this need. In contrast to the present need for wide-frequency-spectrum radar antennas, the IFF requirements were less stringent in terms of beam shape in the elevation plane, bandwidth, and power-handling capacity. The interrogators used for IFF operated in a relatively narrow frequency band of about ±3 percent. Since the elevation position of the target to be interrogated is known from the radar data, a fan beam in that plane is sufficient to give the required data. Although specifically designed for the IFF band, many of the SAMB components maintain satisfactory characteristics over at least a 25 percent frequency band. Hence, the techniques can be used for other frequency bands and configurations. The wideband capability of the SAMB antenna is of particular interest for the wide-spectrum cylindrical array for the radar application.

## Radiating Array

The SAMB antenna is one side of a proposed four-sided configuration, each side a planar array which scans ±45° from broadside in azimuth to give 360° coverage. It consists of 32 elements in the horizontal plane and two elements in the vertical plane. The radiating elements are of the logarithmic trapezoidal-tooth (LTT) type and have been widely investigated. Figure 2 shows a portion of the array with the elements. The ±45° scan sector is covered by from 28 to 32 discrete beams which can be scanned sequentially or by jump-scanning with a high beam agility. The average beamwidth is on the order of 5° in azimuth and 35° in elevation.

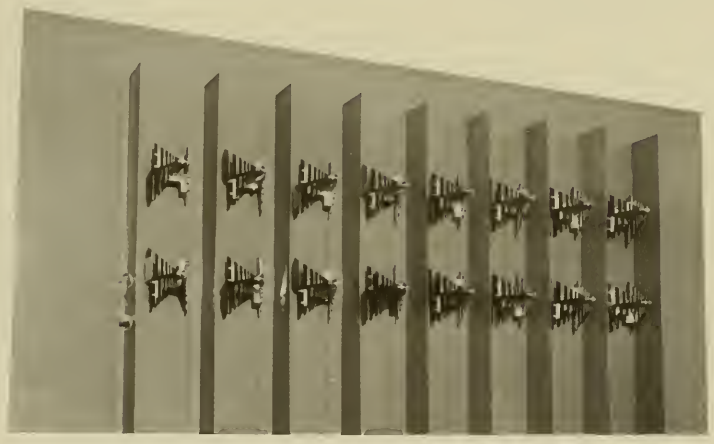

Figure 2. Section of SAMB radiating array.

## Beam Forming And Steering

Two approaches were used to produce the desired amplitude and phase at the element terminals on the SAMB antenna: one employing a matrix, and the other, true-time-delay lines. A Taylor distribution in amplitude that would yield side lobes on the order of -27 dB was chosen.

A 32-port matrix[4] was designed and constructed under contract by Radiation Systems, Inc., Alexandria, Virginia. This matrix is capable of producing a single beam at a given angle for each input terminal excited, or will yield simultaneous multiple beams if all of the input terminals are excited simultaneously. The device is so constructed that the correct amplitude and phase are applied to the antenna terminals to provide for 28 different beam positions. A diode switching matrix developed by NELC allows sequential or jump scanning as desired. Figure 3 shows this system in block diagram. Details of the matrix switches are given in reference 5.

The true-time-delay system for amplitude and phase control was designed and constructed under contract to Sylvania Electronic Systems, Waltham, Massachusetts. This method employed a 1:32 power divider to yield the Taylor amplitude distribution. Each of the 32 output ports of the power divider was connected to a five-bit time-delay board consisting of 32 possible true-time-delay path lengths for each element. Programmed microwave diode switches were used to select the proper line length to give a selected beam direction. Figure 4 shows this system in block diagram.

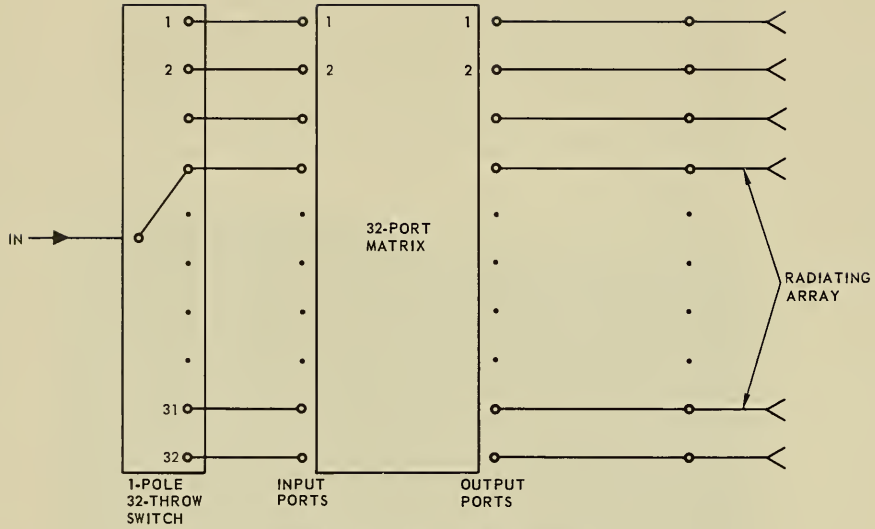


Figure 3. Matrix system for SAMB antenna.

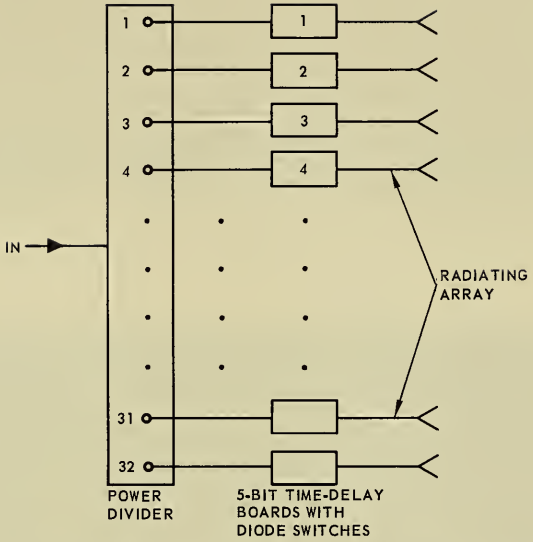


Figure 4. True-time-delay system for amplitude and phase control, SAMB antenna.

Each of the two methods described has advantages and disadvantages which depend on the application desired. A distinct advantage of the true-time-delay technique is that the beam position does not shift as the frequency is changed, as is the case for the matrix approach. The beam-position shift is dramatically illustrated in figure 5 which gives the experimental radiation patterns of the SAMB matrix antenna for different beam positions. Beams 1L and 1R are near the broadside position, beams 7L and 7R are about 22° off broadside, and beams 14L and 14R are about 50° off broadside. As is evident, the effect is more pronounced as the beam is scanned to larger angles. Over a wide-frequency spectrum, this condition would give large angular differences between the transmitted and received signals when they are separated in frequency. This effect is also present when phase-increment scanning is used and will be discussed later. If many beam positions are desired simultaneously, then the matrix-feed technique has a definite advantage over other feed systems. Measured radiation patterns for the SAMB true-time-delay antenna are shown in figures 6, 7, and 8 for two frequencies separated by about 3 percent. Beams 1L, 6L, and 16L are shown and no beam-position shift is observed for any beam.

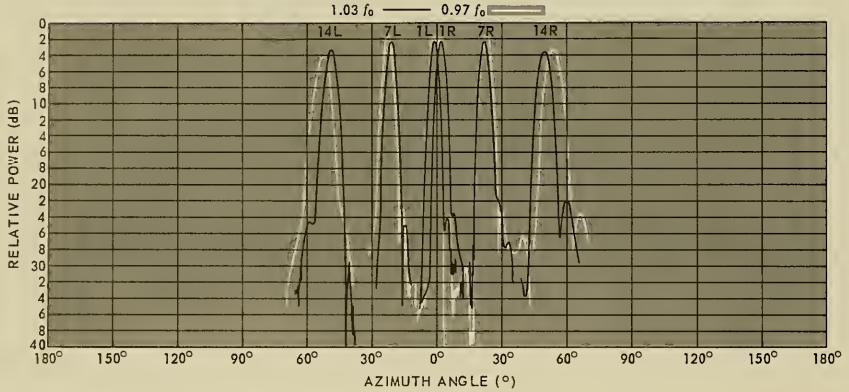


Figure 5. SAMB beam-position shift with frequency using matrix.

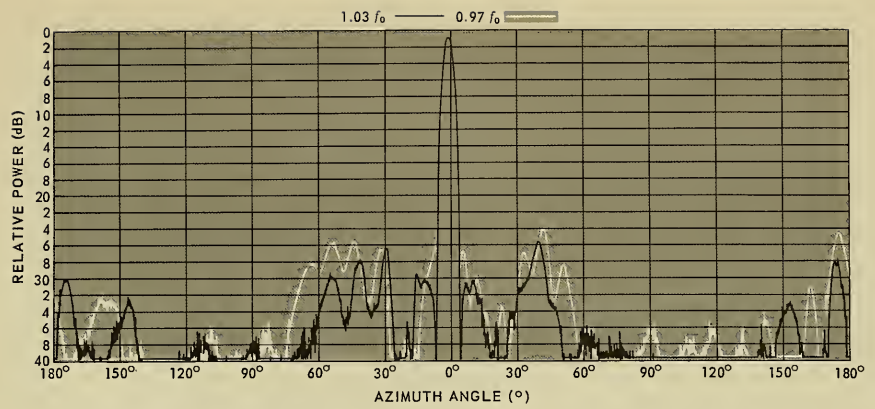


Figure 6. SAMB time-delay pattern, beam 1L, 0.97 $f_0$, 1.03 $f_0$.

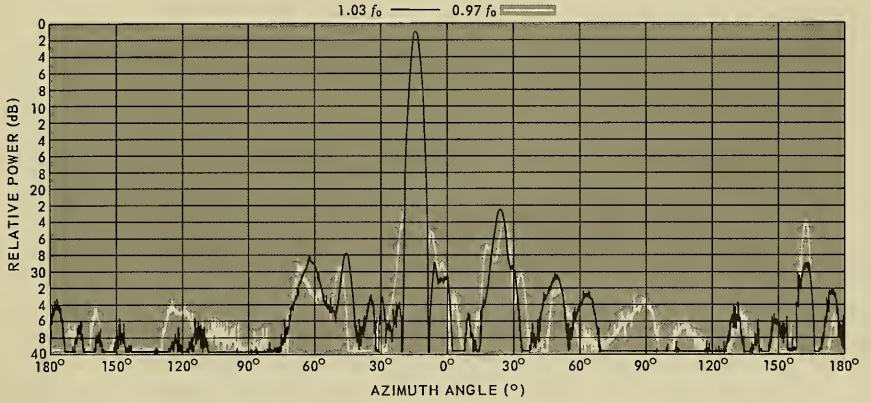


Figure 7. SAMB time-delay pattern, beam 6L, 0.97 $f_0$, 1.03 $f_0$.

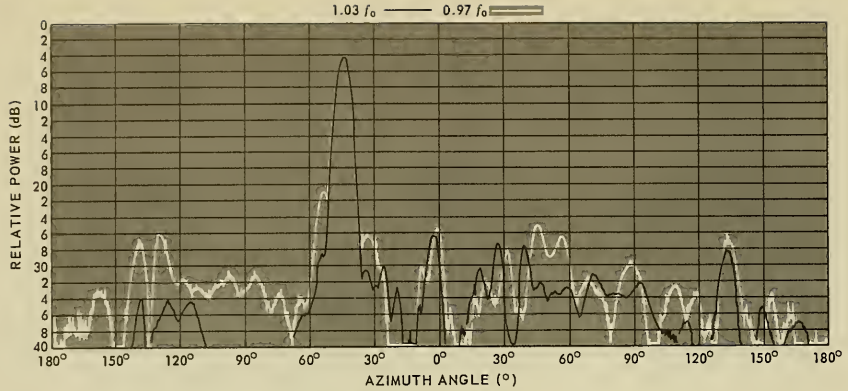


Figure 8. SAMB time-delay pattern, beam 16L, 0.97 $f_0$, 1.03 $f_0$.

The SAMB antenna system was implemented with the Mark X IFF system and driven by a digital computer to scan over the ±45° sector to track random targets of opportunity.

## Experimental Radiation Patterns, SAMB Matrix Feed

Typical patterns for various beam positions over a 30 percent frequency band are shown in figures 9 through 23. It is observed that the side-lobe level increases rather quickly when the frequency is changed beyond ±10 percent of the design frequency for the various beam positions. The beam-position shift due to frequency results in about 15° shift over the 30 percent band for beam 14L, the position of which at the design frequency is 52°. Similar results are also present for the other beam positions, but at a magnitude proportional to the angle off broadside and to the frequency increment. Figure 24 shows a composite pattern of all beams giving full 45° sector coverage. Note that 14 beams adequately cover the scanning sector.

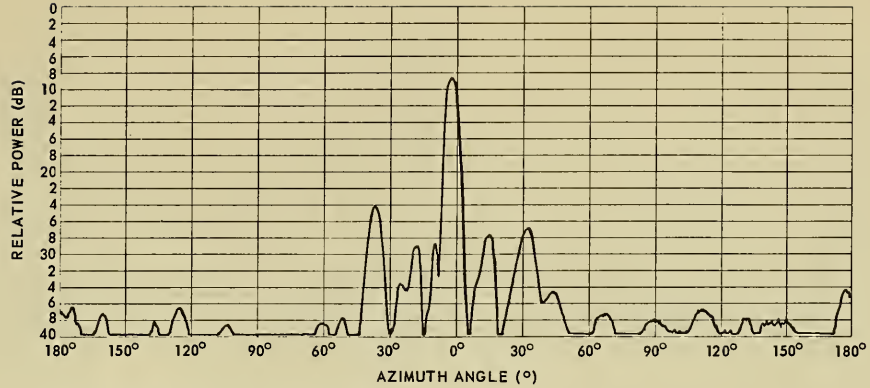


Figure 9. SAMB matrix-array pattern, beam 1L, 0.80 $f_0$.

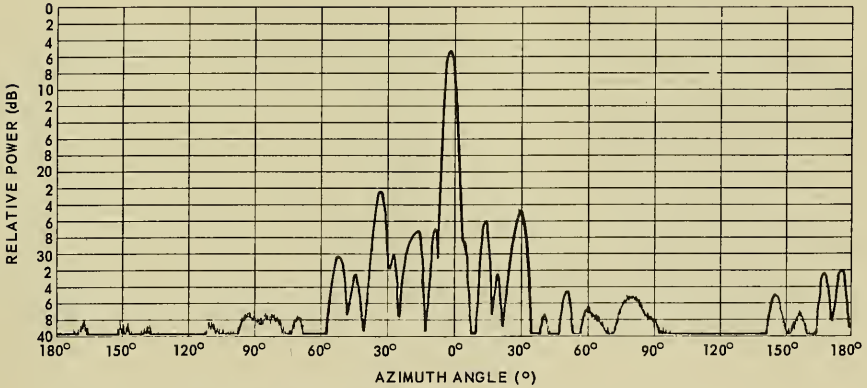


Figure 10. SAMB matrix-array pattern, beam 1L, 0.90 $f_0$.

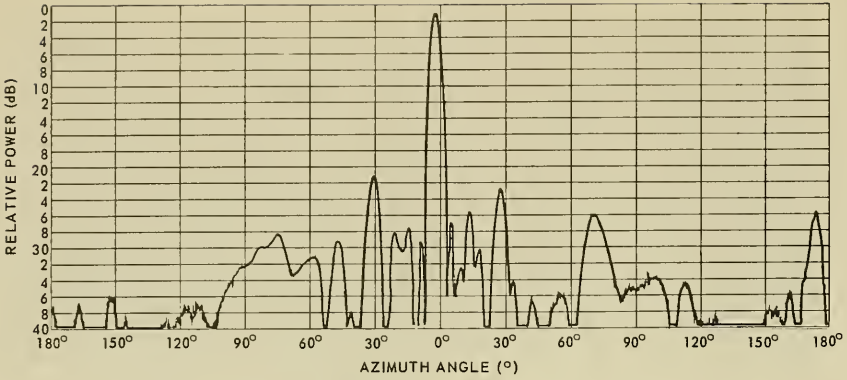


Figure 11. SAMB matrix-array pattern, beam 1L, 0.95 $f_0$.

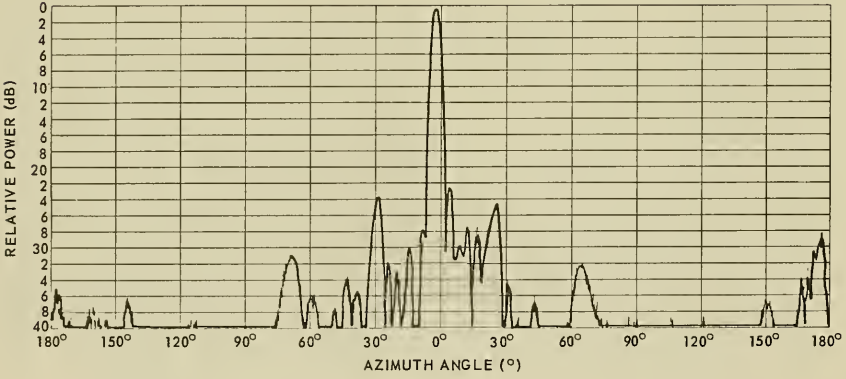


Figure 12. SAMB matrix-array pattern, beam 1L, $f_0$.

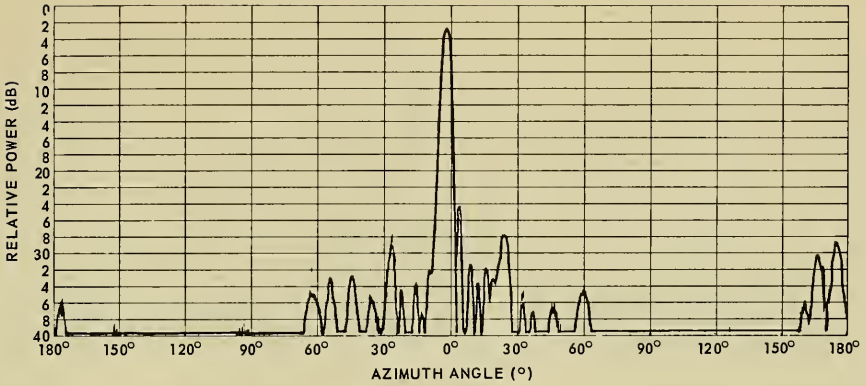


Figure 13. SAMB matrix-array pattern, beam 1L, 1.10 $f_o$.

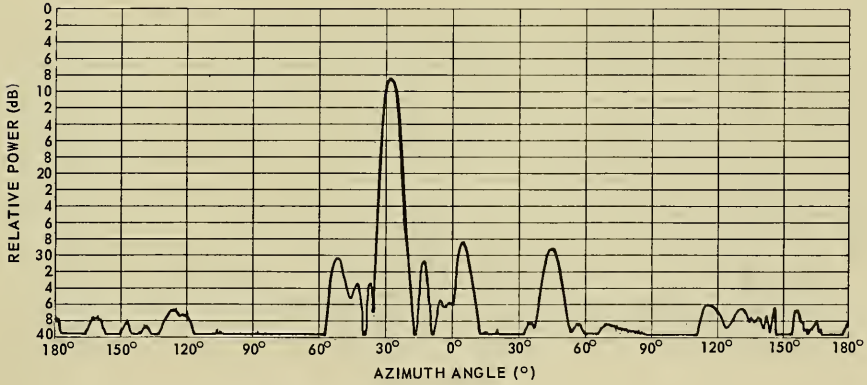


Figure 14. SAMB matrix-array pattern, beam 7L, 0.80 $f_o$.

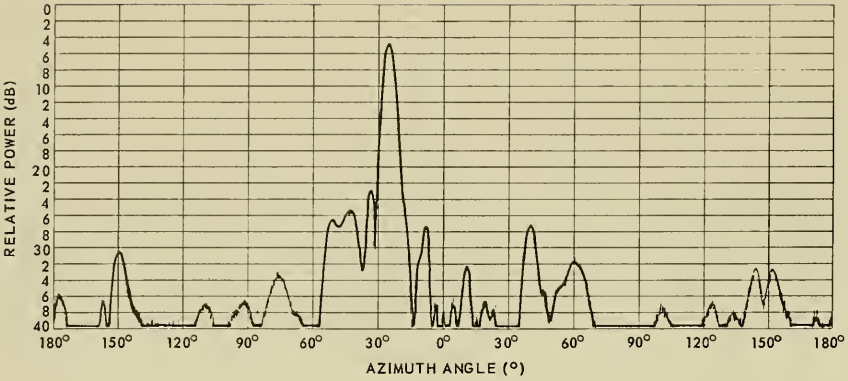


Figure 15. SAMB matrix-array pattern, beam 7L, 0.90 $f_0$.


Figure 16. SAMB matrix-array pattern, beam 7L, 0.95 $f_0$.

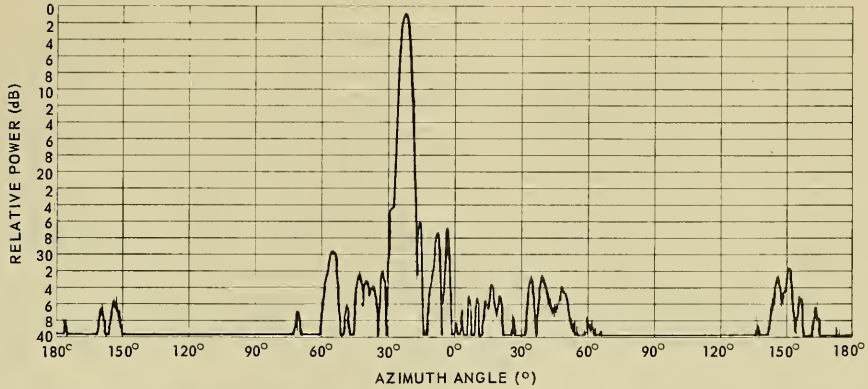


Figure 17. SAMB matrix-array pattern, beam 7L, $f_0$.

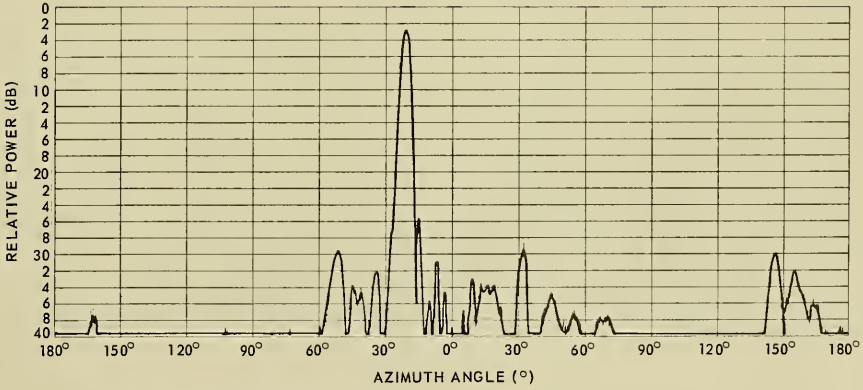


Figure 18. SAMB matrix-array pattern, beam 7L, 1.10 $f_0$.

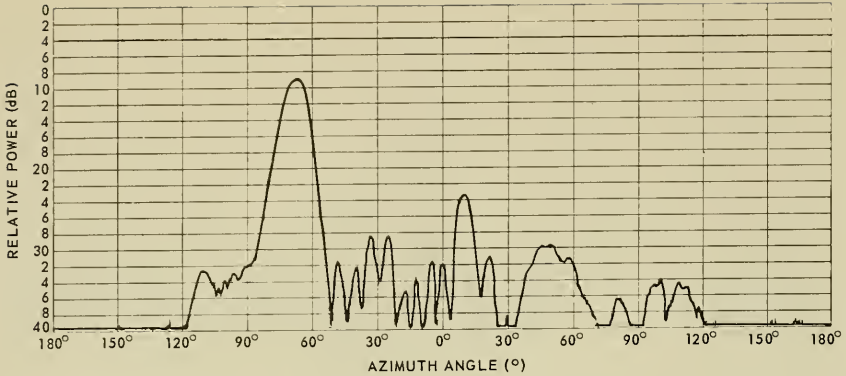


Figure 19. SAMB matrix-array pattern, beam 14L, 0.80 $f_0$.

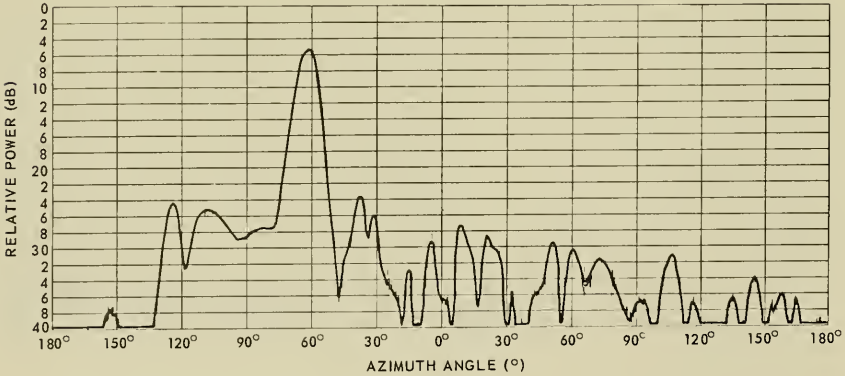


Figure 20. SAMB matrix-array pattern, beam 14L, 0.90 $f_0$.

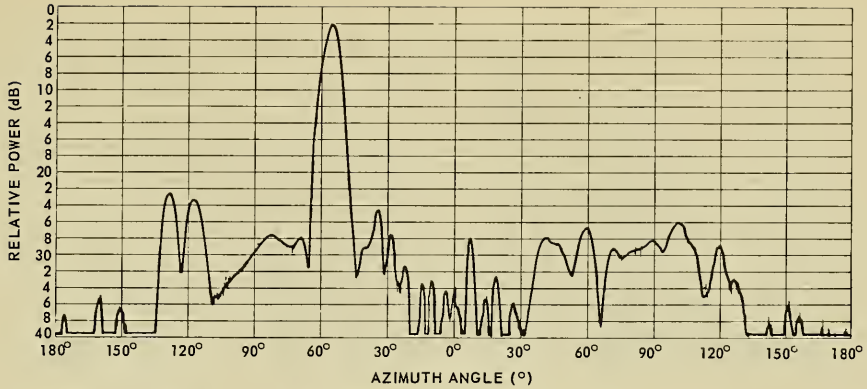


Figure 21. SAMB matrix-array pattern, beam 14L, 0.95 $f_0$.

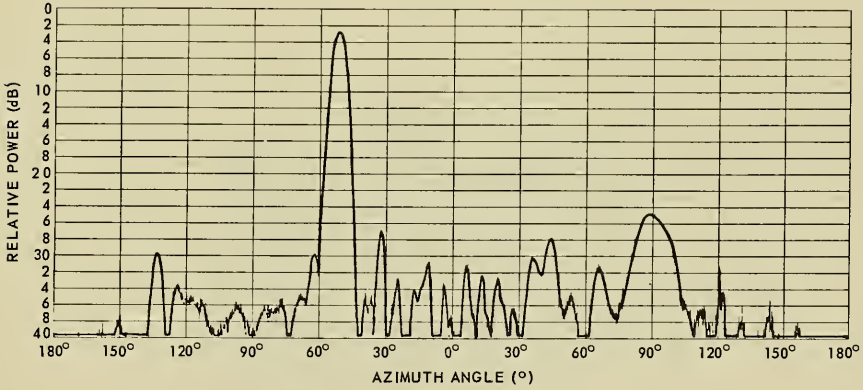


Figure 22. SAMB matrix-array pattern, beam 14L, $f_0$.

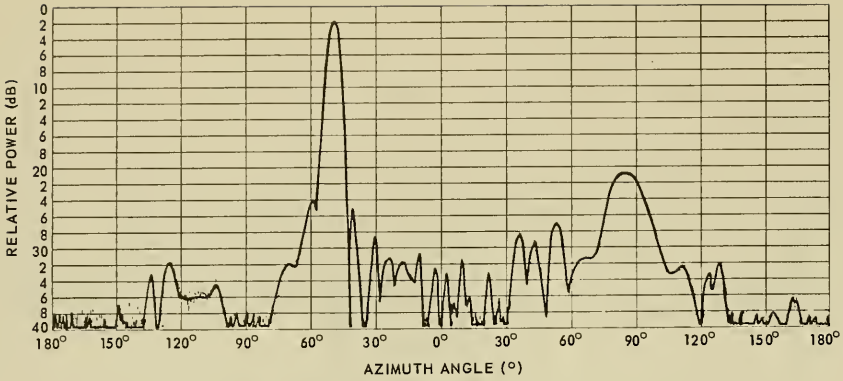


Figure 23. SAMB matrix-array pattern, beam 14L, 1.05 $f_0$.

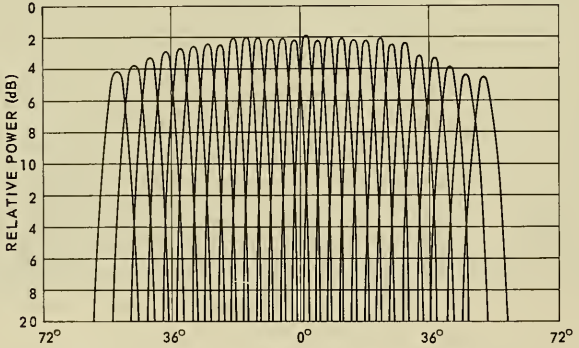


Figure 24. SAMB matrix-array patterns, 45° aector coverage, $f_0$.

## Experimental Radiation Patterns, SAMB Time-Delay System

A composite pattern of the 32 beams of the true-time-delay system is shown in figure 25. Note that in this case 32 beams are required to adequately cover the sector, since less beam-broadening occurs for this system. These patterns were taken over a 50-percent frequency band, to permit determining the extent of pattern deterioration with bandwidth. Figures 26 through 44 show beam 1L near broadside and beam 16L approximately 45° off broadside. Figures 27 through 33 show that beam 1L has side lobes no higher than -20 dB over about a 40-percent band, and that there is little deterioration in the main beam shape. Beam 16L, as shown in figures 36 through 40, has side lobes lower than -20 dB over only a 25-percent frequency band, and the beam deteriorates rapidly beyond the limits of 0.8 $f_0$ and 1.05 $f_0$. Note, however, that the position for a given beam is constant over the frequency range, a characteristic of the true-time-delay method of scanning.

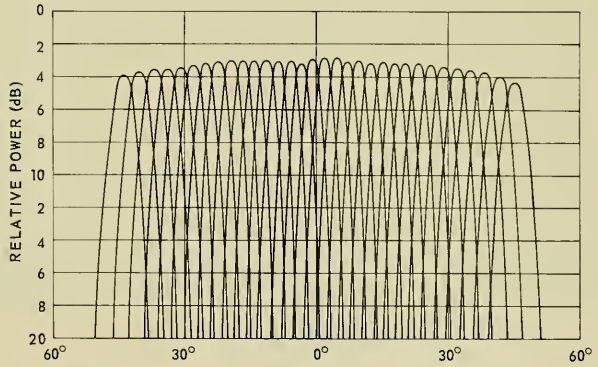


Figure 25. SAMB time-delay array patterns, 45° sector coverage, $f_0$.

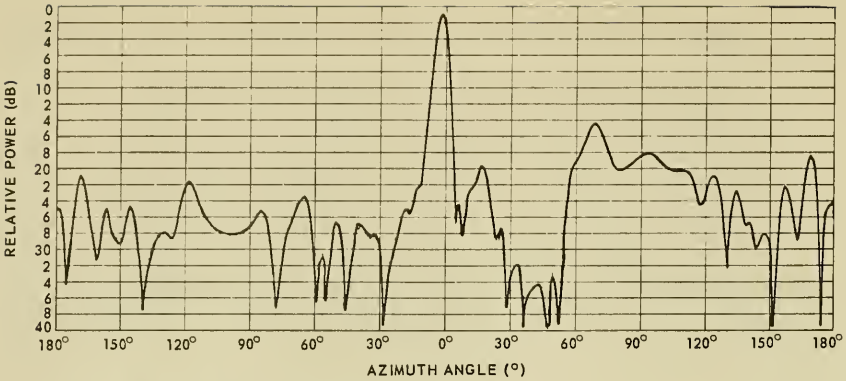


Figure 26. SAMB time-delay pattern, beam 1L, 0.75 $f_0$.

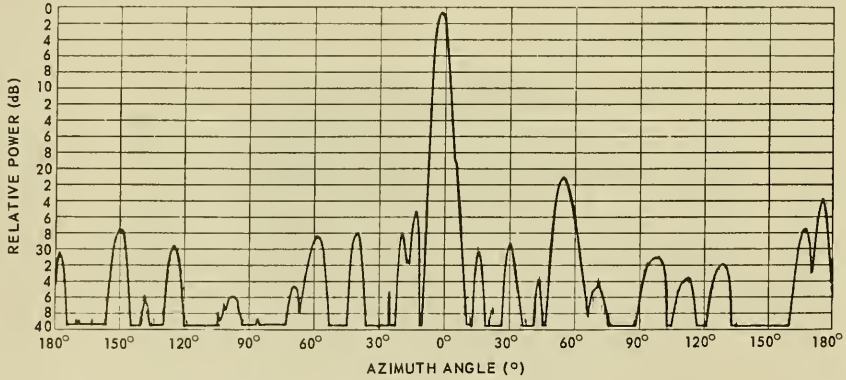


Figure 27. SAMB time-delay pattern, beam 1L, 0.80 $f_0$.

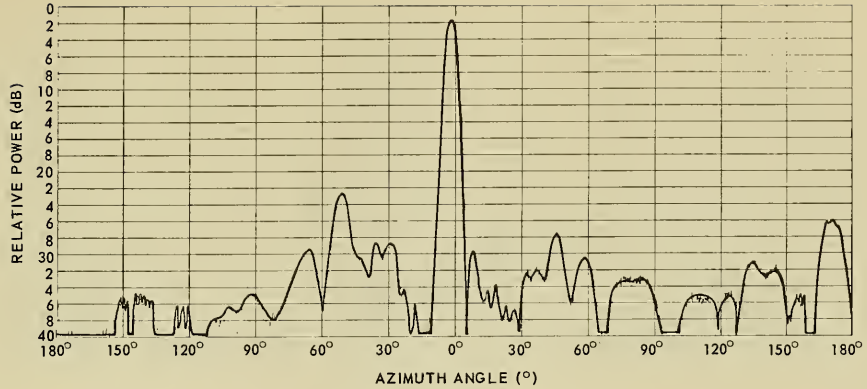


Figure 28. SAMB time-delay pattern, beam 1L, 0.90 $f_0$.

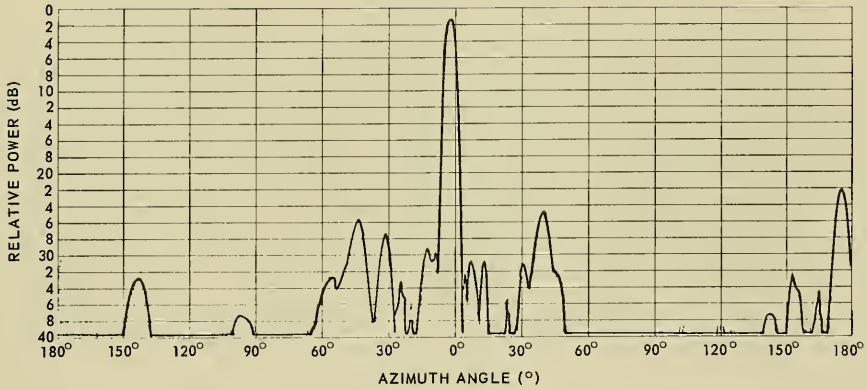


Figure 29. SAMB time-delay pattern, beam 1L, $f_0$.

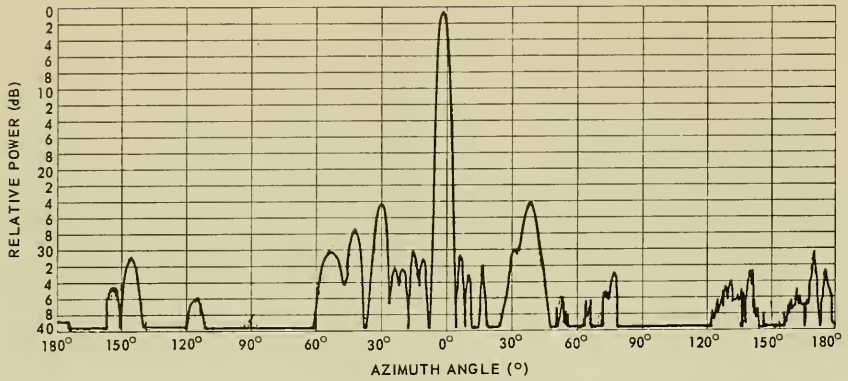


Figure 30. SAMB time-delay pattern, beam 1L, 1.05 $f_0$.

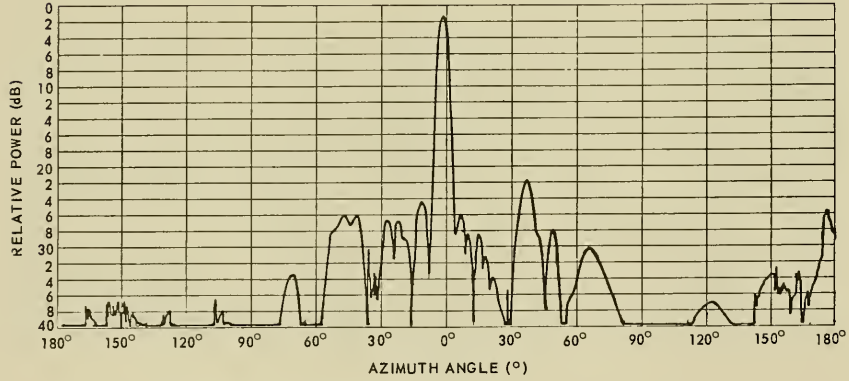


Figure 31. SAMB time-delay pattern, beam 1L, 1.10 $f_0$.

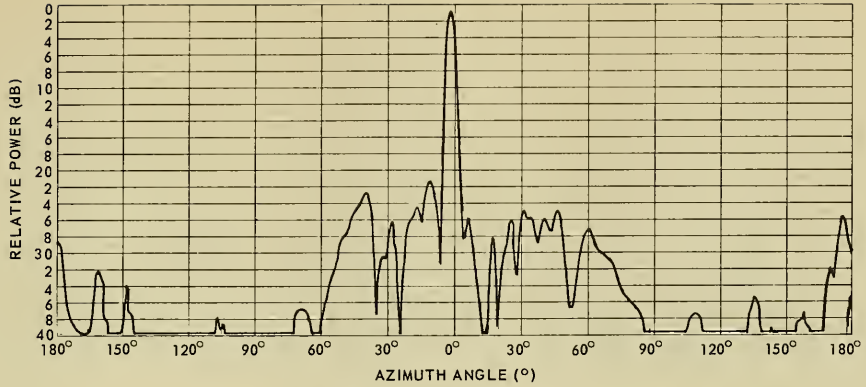


Figure 32. SAMB time-delay pattern, beam 1L, 1.15 $f_0$.

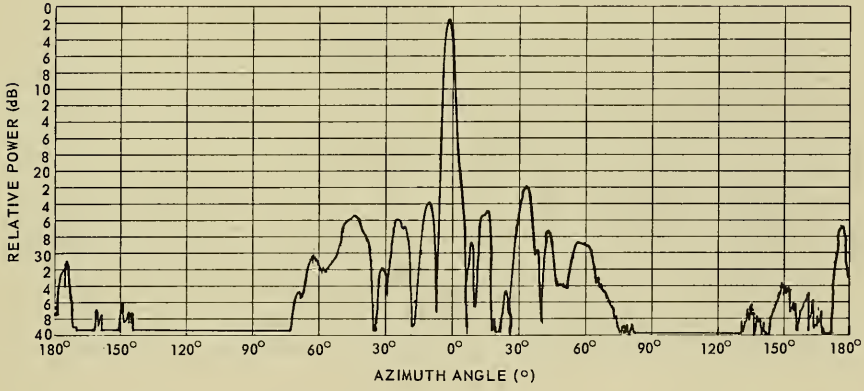


Figure 33. SAMB time-delay pattern, beam 1L, 1.20 $f_0$.

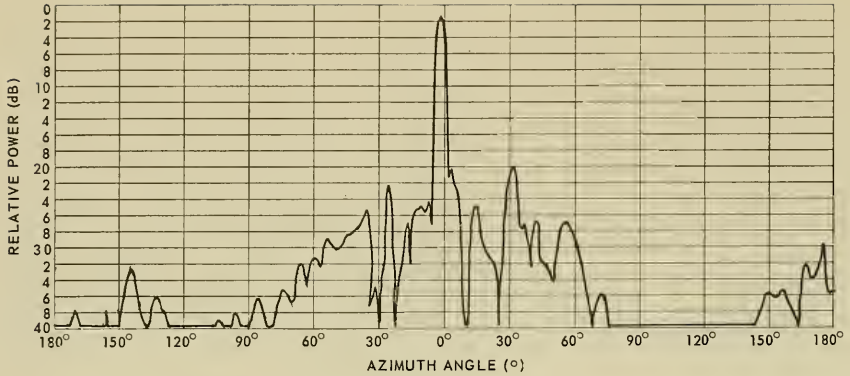


Figure 34. SAMB time-delay pattern, beam 1L, 1.25 $f_0$.

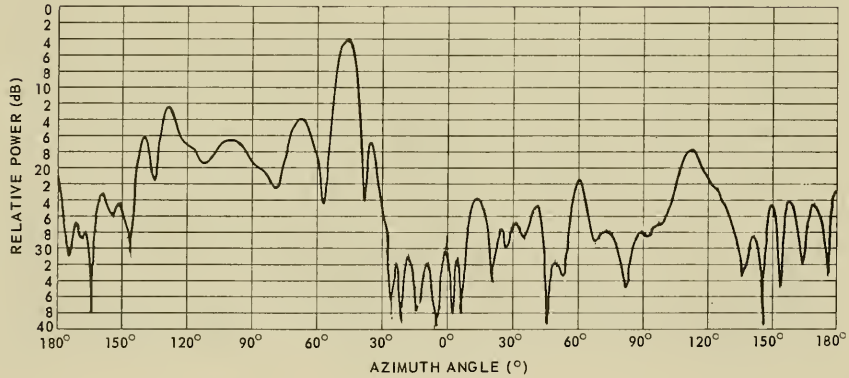


Figure 35. SAMB time-delay pattern, beam 16L, 0.75 $f_0$.

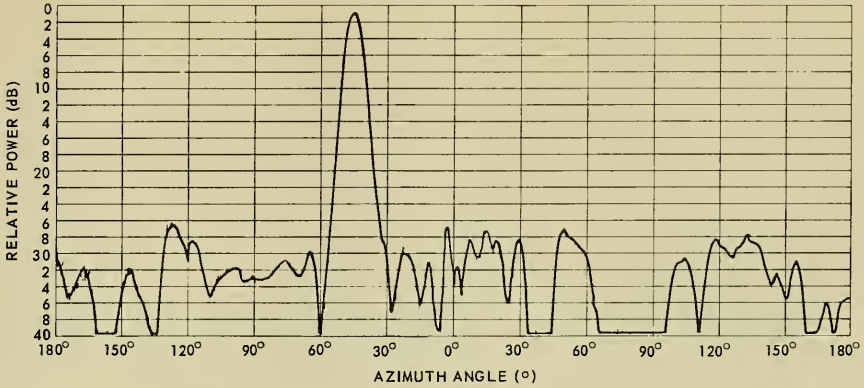


Figure 36. SAMB time-delay pattern, beam 16L, 0.80 $f_0$.

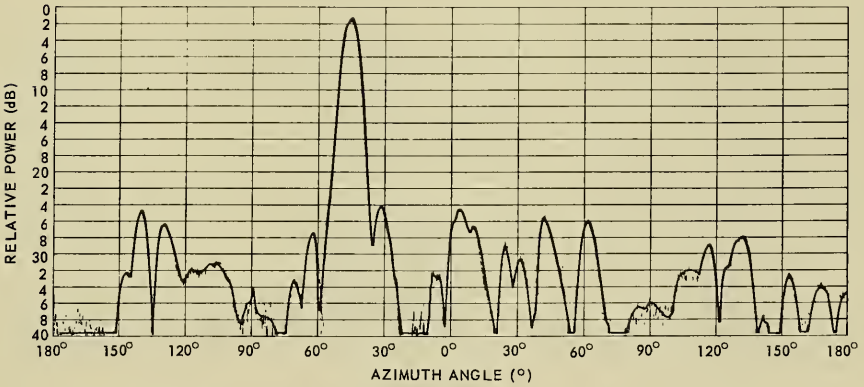


Figure 37. SAMB time-delay pattern, beam 16L, 0.85 $f_0$.

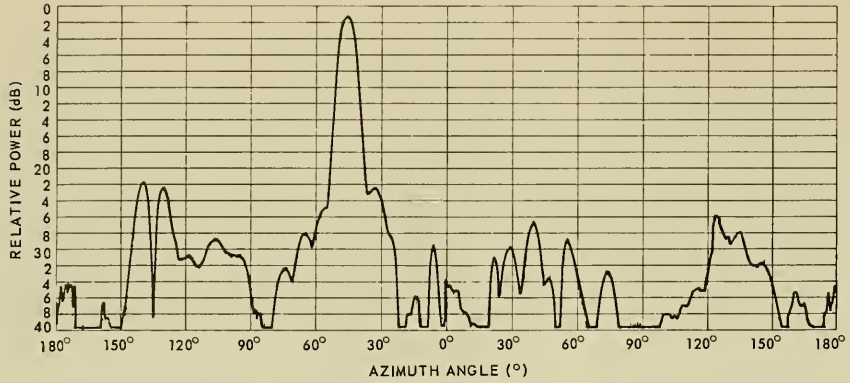


Figure 38. SAMB time-delay pattern, beam 16L, 0.90 $f_0$.

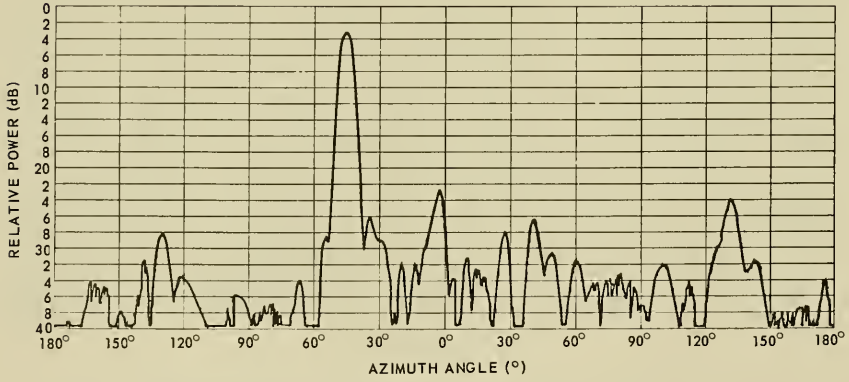


Figure 39. SAMB time-delay pattern, beam 16L, $f_0$.

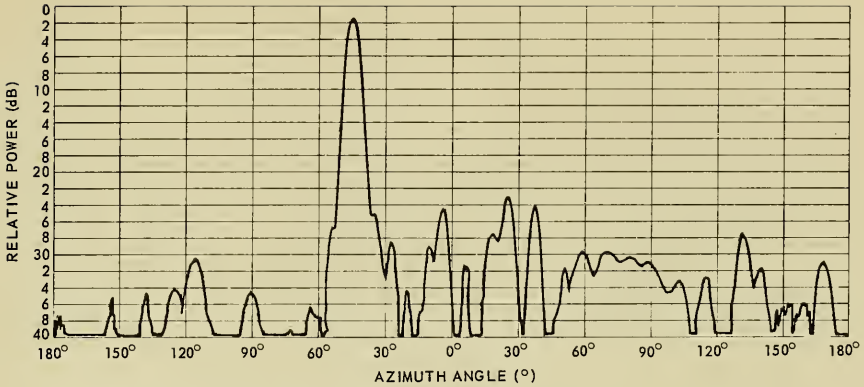


Figure 40. SAMB time-delay pattern, beam 16L, 1.05 $f_0$.

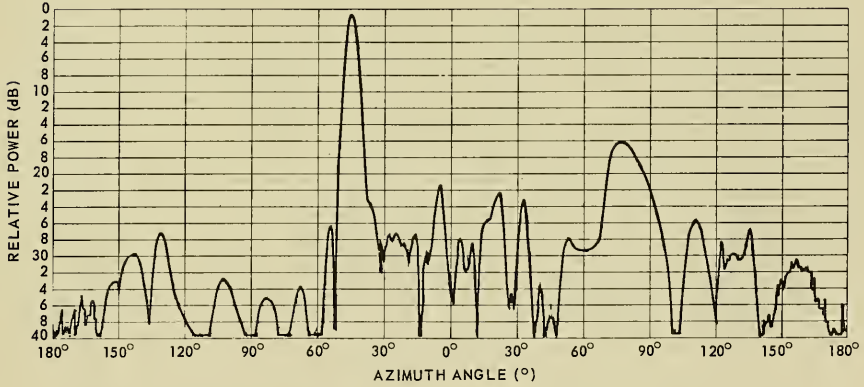


Figure 41. SAMB time-delay pattern, beam 16L, 1.10 $f_0$.

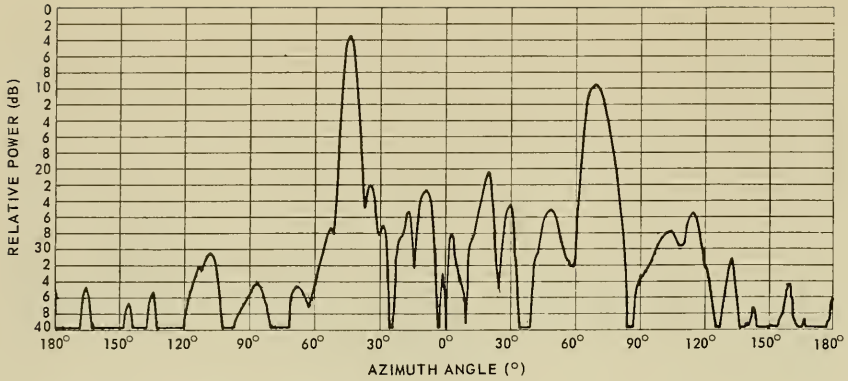


Figure 42. SAMB time-delay pattern, beam 16L, 1.15 $f_0$.

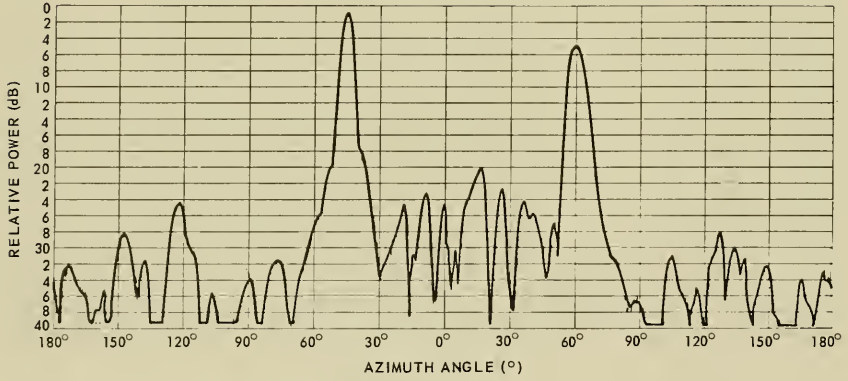


Figure 43. SAMB time-delay pattern, beam 16L, 1.20 $f_0$.

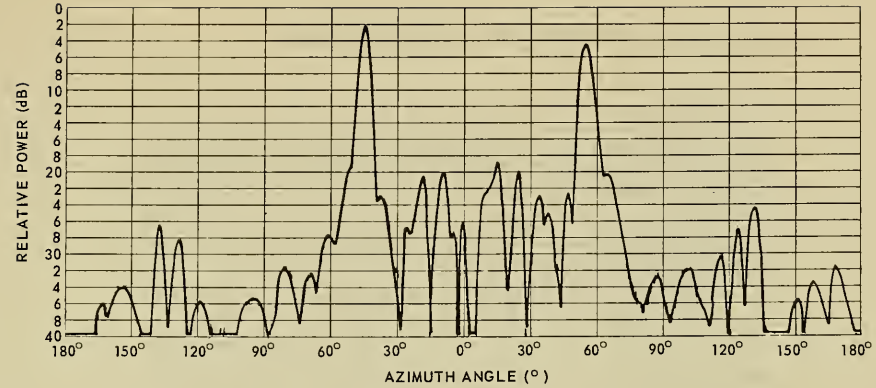


Figure 44. SAMB time-delay pattern, beam 16L, 1.25 $f_0$.

## Discussion Of SAMB Radiation Patterns

Some general conclusions can be drawn from the analysis of the SAMB antenna-radiation patterns.

1. Beam-position shift with frequency occurs for systems not using true-time-delay beam-steering techniques. Approximately 15° shift is observed for scan angles on the order of 45° in the matrix-fed system over a 30-percent frequency band.

2. The true-time-delay method exhibits good radiation-pattern behavior over the 30-percent frequency band, and for all scan angles less than $\pm 45°$. Side-lobe levels remain under -20 dB and main beam shape is maintained

3. If the scan angle is decreased, then the usable frequency bandwidth for the time-delay method is increased.

4. The bandwidth of the matrix method is less than that of the time-delay method with respect to side-lobe level and main-beam shape. The side lobes remain under -20 dB for about a 15-percent band. However, since the development of the systems described, advances in the design of the hybrid matrix have extended the usable bandwidth of a matrix to well over an octave Hence, the matrix cannot be ruled out for wideband applications.

5. When simultaneous multiple beams are desired, the matrix offers an excellent method for achieving them.

# THE CARAMBA ANTENNA

The CARAMBA program has been concerned with investigating techniques of scanning a fan beam. Since the elevation pattern of the fan beam is the pattern of an individual element in that plane, stacking of ring arrays results in the pencil beam or, alternatively, a ring array using linear arrays parallel to the cylinder axis as elements can produce the same pencil beam. Of concern here are methods of beam-forming and phasing to obtain pencil beams from a cylindrical configuration of elements, and the results of the CARAMBA program can be of use for this goal.

The CARAMBA antenna consists of a ring array of 128 sectorial horns embedded in a metallic cylinder of 13 wavelengths, fed by two methods:

1. A unique lens-feed system which permits application of amplitude taper to the array element terminals, and

2. A digital amplitude and phase board which allows a variety of amplitude and phase distributions to be applied to the terminals.

## CARAMBA I

The lens-feed and radiating-array system is designated as CARAMBA I.[3] The lens is a parallel-plate R-2R device which places the correct phases at the array elements when the lens and array radii are in a 1:2 ratio. Placed about one-quarter wavelength from the lens periphery are 64 input-output probes. Four of the probes are used simultaneously as inputs, and fed with a 1-2-2-1 amplitude taper. The lens output probes for 32 elements are connected to the radiating elements by means of equal-length cables.[3,6] By feeding more than one of the input probes at one time, the energy propagated through the lens is highly directive, and is removed at the diametrically opposite output probes with a taper, to produce low side lobes in the radiation pattern of the array. A typical array schematic is shown in figure 45 and radiation patterns for a four-probe tapered input are given in figure 46. The beam is scanned in azimuth by means of diode switches at each lens port and by additional circuitry to maintain the proper input-probe taper. The system is operable over a 20-percent frequency band.

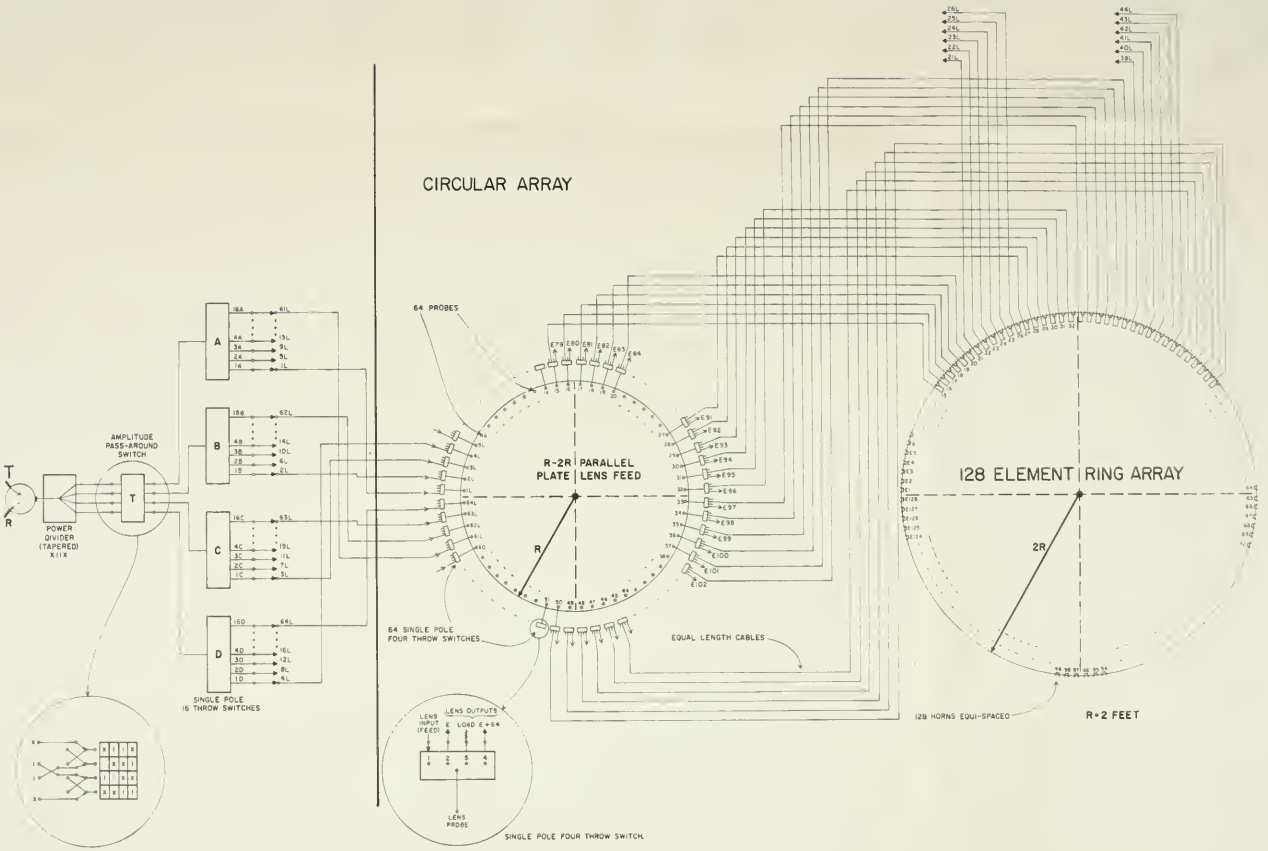


Figure 45. CARAMBA I system schematic.

REVERSE SIDE BLANK

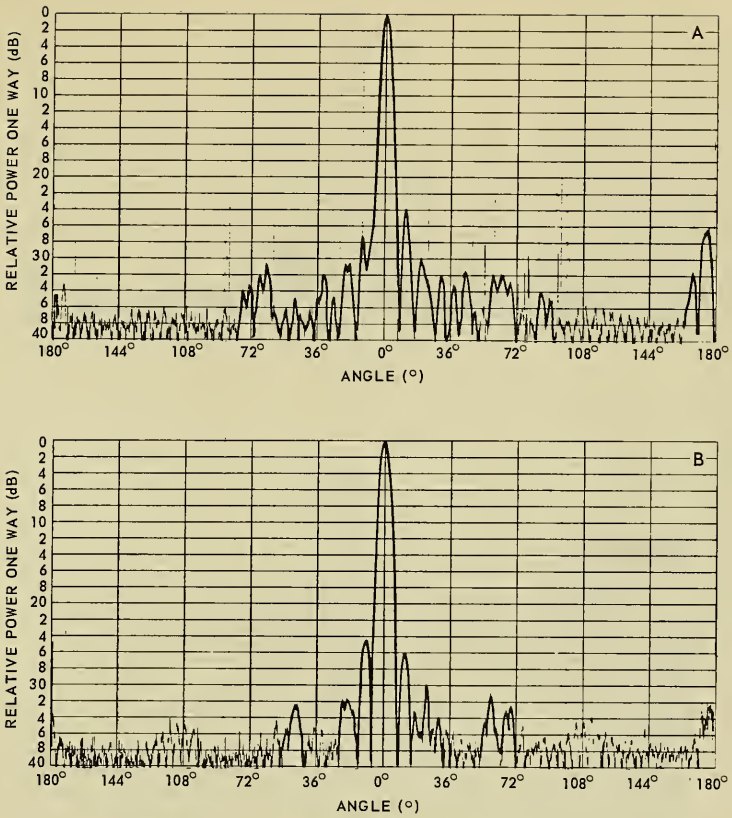


Figure 46. CARAMBA I radiation patterns, 32-element array, 4-probe feed, tapered 6 dB. A, 0.91 $f_0$. B, $f_0$. C, 1.09 $f_0$.

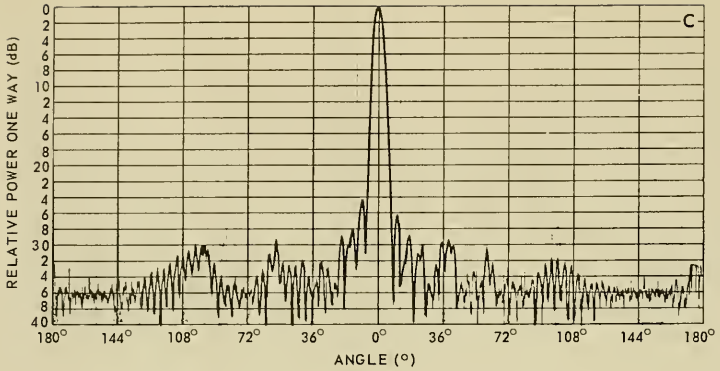


Figure 46 (Continued).

## CARAMBA II

CARAMBA II consists of the radiating array described above, and is fed by means of 32 three-bit amplitude and phase boards through a 1:32 uniform power divider. This allows eight different amplitudes and eight different phases to be applied to each array element, thus giving many possible amplitude and phase distributions across the array aperture. The system is shown schematically in figure 47 and a typical pattern is shown in figure 48. Some pattern deterioration is observed near the ends of a 20-percent frequency band, but the results can be improved by phase-trimming techniques presently under study. A computer prediction of side-lobe level gave about -17 dB using the three-bit phase and amplitude distributions implemented on the array. The phase quantization approximation contributes a large factor to the relatively high side lobes. The system is scanned through 360° in azimuth using a four-pole switch to select elements in each of the four quadrants.

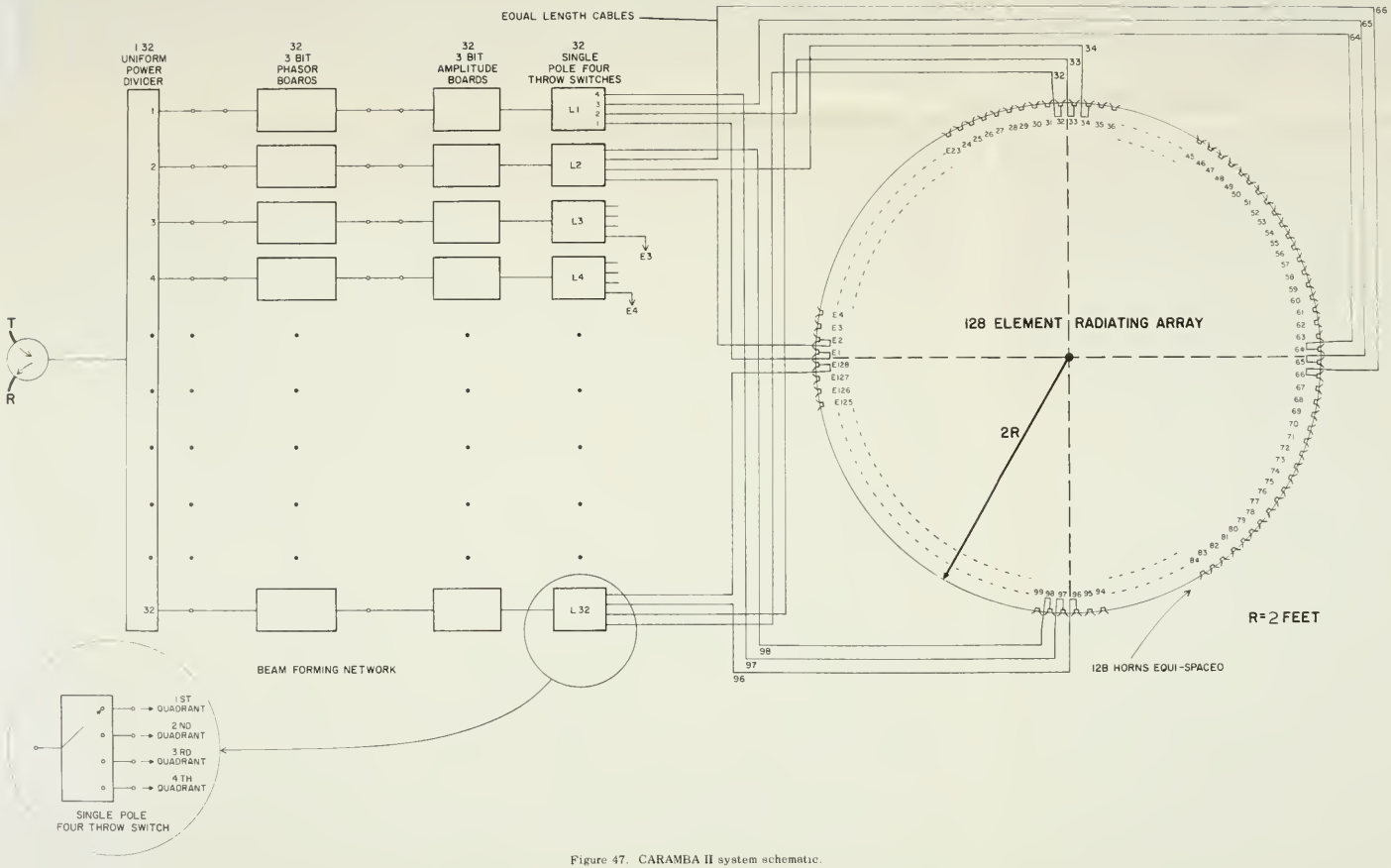


Figure 47. CARAMBA II system schematic.

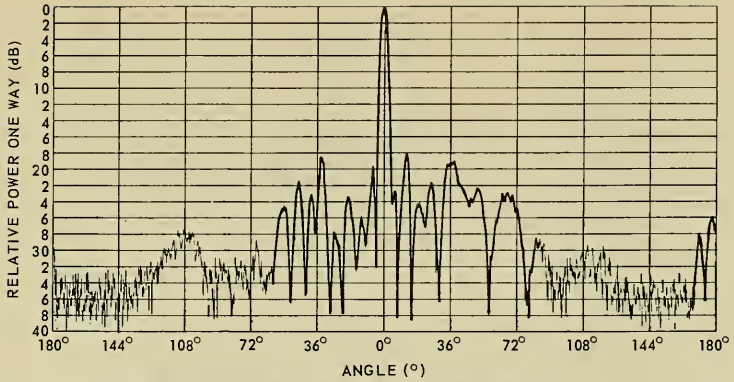


Figure 48. CARAMBA II azimuth pattern, 3-bit phase-board feed, $f_0$.

Some conclusions can be drawn from the results of the CARAMBA program:

1. Low-side-lobe, circular-array antenna patterns can be achieved using the R-2R lens fed with four input probes to obtain a tapered output distribution. Side lobes on the resulting radiation patterns are on the order of -25 dB over a 20-percent frequency band.

2. The use of digital amplitude and phase distributions obtained by means of diode techniques gives radiation patterns which can be predicted by computer techniques, within the system errors.

3. The digital method is valuable as a research tool. Many combinations of amplitude and phase distributions can be readily placed on the element terminals by means of amplitude and phase-control panels.

As an example of the versatility of the digital method, figure 49 shows the difference pattern obtained from the array by simply advancing the phase-control switches on the panel 180°. Strictly speaking, independent control of the digital amplitude and phase is not possible, since a change of the amplitude bit results in a slight change of the phase, because of the physical construction of the phasor

board. This is not considered serious, since on the final system the amplitude would remain fixed after the optimum value has been determined. Another effect is observed if all of the phases are advanced by the same value: since the number of phase errors between bits is not the same for all bits, changes in the radiation pattern occur as the beam is scanned through 360°. This effect will also be minimized if a phase-trimming scheme is used in the system. As in the case of the matrix previously discussed, the phasor board is a discrete phase-step device and will be subject to changes in beam-pointing direction as the frequency is changed. This is not a serious problem for the circular array, but for elevation scanning it would be a factor to be investigated.

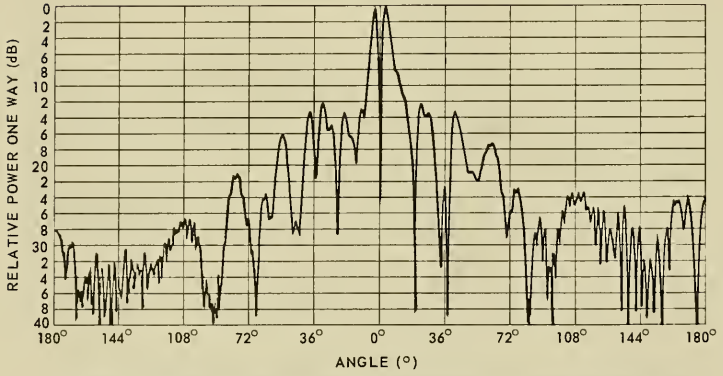


Figure 49. CARAMBA II azimuth difference pattern obtained by advancing phase-control switches 180°, 0.95 $f_0$.

# APPLICATIONS OF THE CYLINDRICAL ARRAY

Cylindrical-array antennas have been used extensively for beacons, TACAN, and other applications where omnidirectional antenna radiation patterns are required. When the omnidirectional pattern was desired, only the constant mode was excited in each ring of elements. However, if a directional beam is desired, all efficient modes must be used. The computation of these modes, or of the related excitation coefficients, is accomplished by means of a high-speed computer. Some of the results of the computation will be discussed later.

The methods of exciting the elements of the configuration vary for the particular application, but for scanning a pencil beam, several techniques have been proposed:

1. The matrix method, which uses a group of matrices to excite the various modes. The beam can be steered by summing the individual modes.

2. The "Wullenweber" method, using a mechanical switching technique to move the beam through 360° in azimuth.

3. The lens-switch technique previously discussed, i.e., CARAMBA I.

4. The use of individual amplitude and phase distribution at each element as previously discussed, i.e., CARAMBA II.

Consider a cylindrical array consisting of a lens feeding a ring of vertical linear arrays as elements, where each element of the linear array is made up of the radiating element and either a digital phasor board or a true-time-delay board to apply the proper phase for elevation scanning. Essentially, this arrangement is a combination of items 3 and 4 above or of item 3 and the SAMB techniques. There is some redundancy because of the lens and the independent phase and amplitude control at the elements. However, the lens is a practical power divider, providing a convenient method of implementing 360° azimuth scanning, and in combination with the digital phasor boards gives a highly versatile research tool for studying the feasibility and limitations of cylindrical elevation scanning of pencil beams. Many of the components developed for CARAMBA I and II can be directly used in the proposed cylindrical array. In addition, other properties of the array can be investigated experimentally, i.e., monopulse, multifrequency, and multifunction techniques.

## Computer Studies

Some important factors in the development of scanning antenna systems are the inherent limitations on desired performance imposed by the geometry of the configuration, and the ability to implement the amplitude and phase distributions required to give the radiation pattern. Computer methods can be used to determine relatively smooth distributions that can be practically implemented, and although they may be somewhat idealized, they are useful in the design of the power-dividing and phasing networks.[7]

The radiation pattern of the cylindrical array can be written

$$E(\varphi,\theta) = \sum_p \sum_q I_{pq} G(\varphi - \alpha_p,\theta) \exp(jqu) \tag{1}$$

where $I_{pq}$ is the excitation of the $p^{\text{th}}$ element in the $q^{\text{th}}$ ring, $G(\varphi - \alpha_p,\theta)$ is the element pattern with the phase referred to the center of the ring, $u = \frac{2\pi}{\lambda} d\sin\theta$, $d$ is the spacing between the rings and $\alpha_p$ is the angular location of the $p^{\text{th}}$ element of any ring. In the present analysis we will consider only current distributions of the form

$$I_{pq} = I^c(\alpha_p) I^e(Z_q) \tag{2}$$

Then (1) can be written

$$E(\varphi,\theta) = E^c(\varphi,\theta) E^e(\theta)$$

where

$$E^c(\varphi,\theta) = \sum_p I(\alpha_p) G(\varphi - \alpha_p,\theta)$$

and

$$E^e(\theta) = \sum_q I(Z_q) \exp(jqu)$$

$E^c(\varphi,\theta)$ is just the ring-array pattern due to a current distribution $I^c(\alpha_p)$ and element pattern $G(\varphi - \alpha_p,\theta)$. $E^e(\theta)$ is the space factor of a linear array with a

current distribution $I^e(Z_q)$. At a beam-pointing angle $\theta_o$, the azimuth pattern is given by $E^c(\varphi,\theta_o)$, and depends only on the distribution $I(\alpha_p)$. The elevation pattern at $\theta_o$ is

$$E^c(\varphi_o,\theta)\,E^e(\theta) \tag{3}$$

and hence depends on both $I^c(\alpha_p)$ and $I^e(Z_q)$. In the direction of the beam, however, the variation of $E(\varphi_o,\theta)$ with $\theta$ is small compared with the variation of $E^e(\theta)$. Thus, for practical purposes, the elevation pattern is completely determined by the distribution $I^e(Z_q)$. This is shown in figures 50-53 which give radiation patterns computed using a 32-element Taylor distribution for $I^e(Z_q)$ and expression (3). As shown by this discussion, it is clear that ring-array techniques are directly applicable to azimuth-beam forming and steering and that linear-array techniques are applicable for elevation-beam steering.

For a beam at $\theta_o$, the required phases of $I^c(\alpha_p)$ and $I^e(Z_q)$ are

$$\Delta^c(\alpha_p) = \frac{2\pi}{\lambda}\rho\cos\theta_o(1-\cos\alpha_p) \tag{4}$$

$$\Delta^e(Z_q) = \frac{2\pi}{\lambda}d\sin\theta_o$$

It should be noted that $\Delta^c(\alpha_p)$ is not essential to pointing the beam at $\theta_o$, but is the phase required to give (approximately) the optimum azimuth pattern at $\theta_o$.

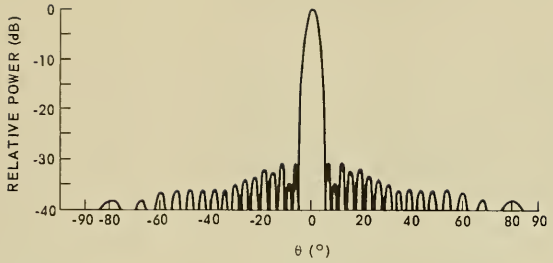


Figure 50. Elevation pattern computed using 32-element Taylor distribution for $I^e(Z_q)$ and expression 3 (p. 47). $\theta_0^{opt} = 0°$; $\theta_0 = 0°$.

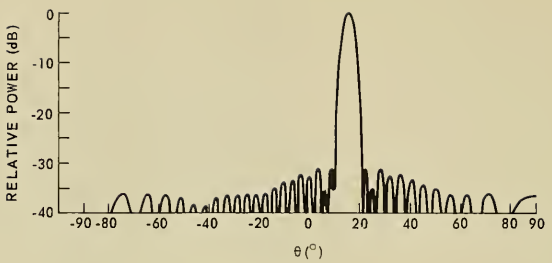


Figure 51. Elevation pattern computed using 32-element Taylor distribution for $I^e(Z_q)$ and expression 3 (p. 47). $\theta_0^{opt} = 0°$; $\theta_0 = 15°$.

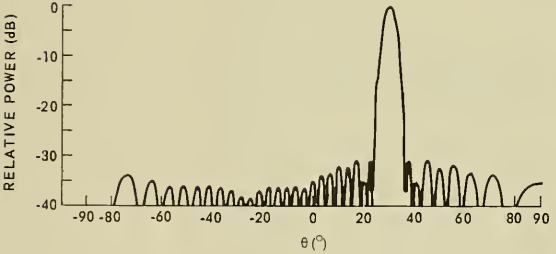


Figure 52. Elevation pattern computed using 32-element Taylor distribution for $I^e(Z_q)$ and expression 3 (p. 47). $\theta_0^{opt} = 0°$; $\theta_0 = 30°$.

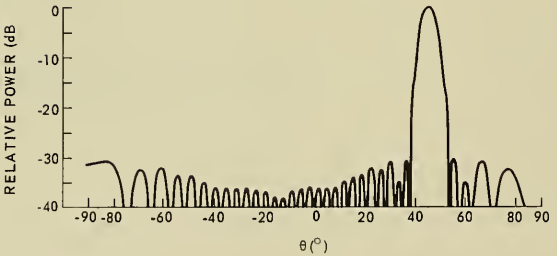


Figure 53. Elevation pattern computed using 32-element Taylor distribution for $I^e(Z_q)$ and expression 3 (p. 47). $\theta_0^{opt} = 0°$; $\theta_0 = 45°$.

For the combination of the CARAMBA and SAMB techniques previously described, only one elevation angle, for example $\theta_o^{opt}$, can be used to determine the optimum distribution $\Delta^c(\alpha_p)$. At other beam-pointing angles, the azimuth pattern will deteriorate from the optimum because of phase errors. The resultant azimuth-pattern beamwidth will broaden, as shown in figures 54 through 61. Figure 62 is a plot of the half-power beamwidth vs elevation angle for various $\theta_o^{opt}$. By choosing $\theta_o^{opt}$ at values other than zero, the useful range of the configuration can be extended, i.e., the azimuth beamwidth can be specified within chosen limits.

Another factor contributing to the beam broadening in azimuth is the decrease in the effective aperture. For comparison to a planar array, one can show that the effective horizontal aperture is $\pi\rho_{eff}$, where $\rho_{eff} = \rho \cos\theta$. Figure 62 shows the beamwidths obtainable with $\theta_o = \theta_o^{opt}$, i.e., the optimum beamwidths possible using the assumed amplitude distribution. It is seen that the beamwidth is indeed broadened by $\cos^{-1}\theta$ as a result of the decrease in effective aperture.

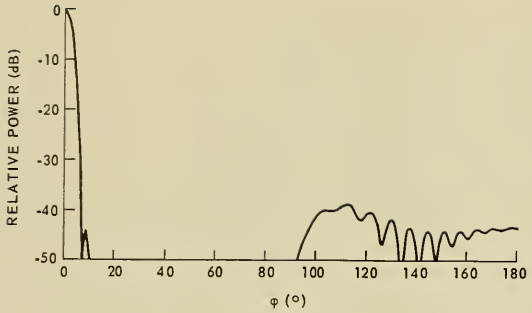


Figure 54. Azimuth pattern, $\theta_0^{opt} = 0$; $\theta_0 = 0$.

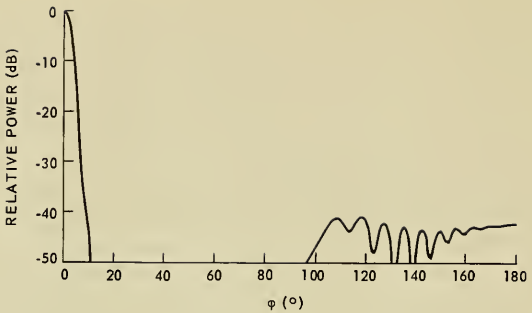


Figure 55. Azimuth pattern, $\theta_0^{opt} = 0$; $\theta_0 = 15°$.

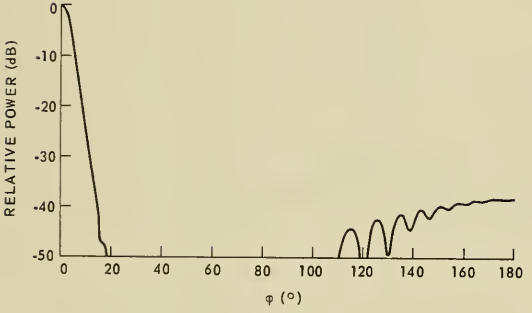


Figure 56. Azimuth pattern, $\theta_0^{opt} = 0°$; $\theta_0 = 30°$.

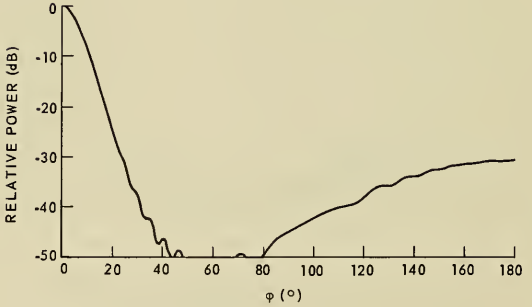


Figure 57. Azimuth pattern, $\theta_0^{opt} = 0°$; $\theta_0 = 45°$.

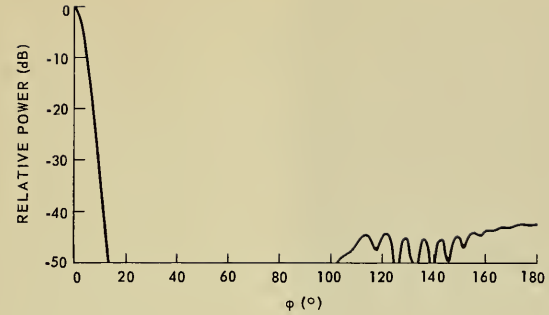


Figure 58. Azimuth pattern, $\theta_0^{opt} = 30°$; $\theta_0 = 0°$.

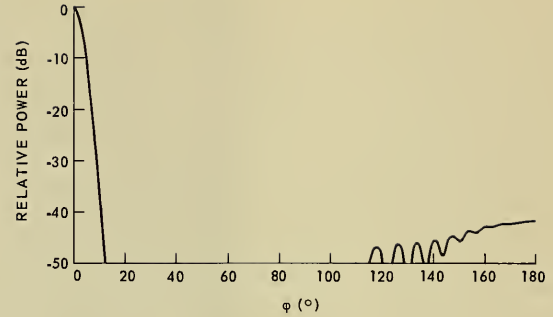


Figure 59. Azimuth pattern, $\theta_0^{opt} = 30°$; $\theta_0 = 15°$.

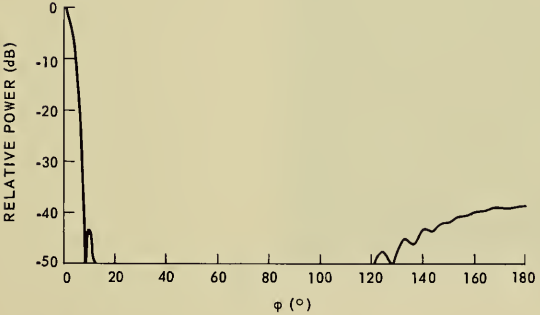


Figure 60. Azimuth pattern, $\theta_0^{opt} = 30°$; $\theta_0 = 30°$.

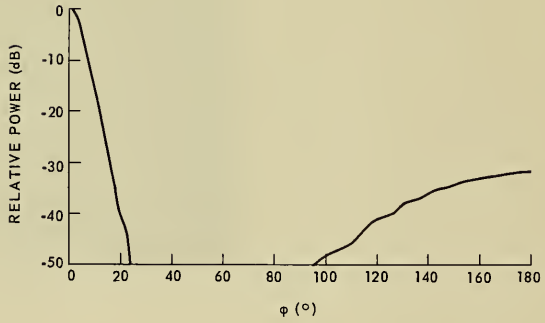


Figure 61. Azimuth pattern, $\theta_0^{opt} = 30°$; $\theta_0 = 45°$.

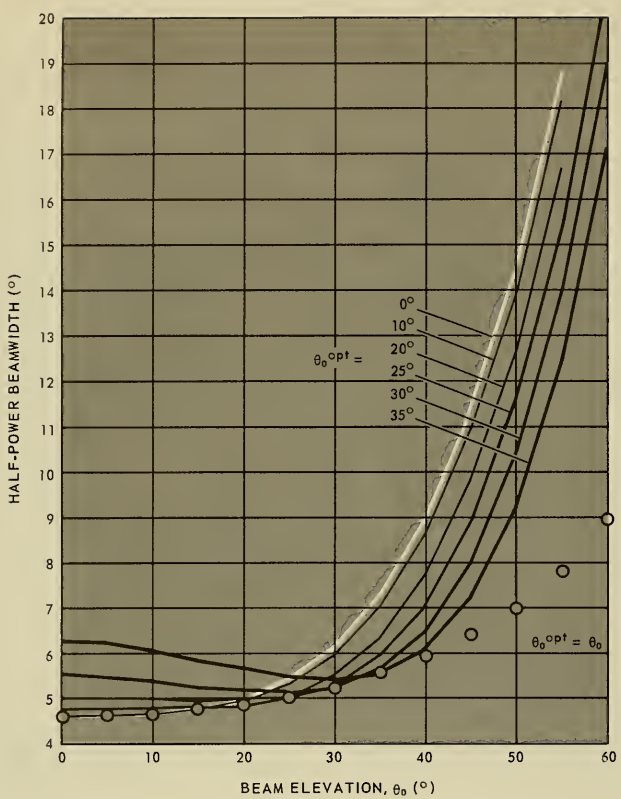


Figure 62. Azimuth half-power beamwidth vs elevation angle, various values of $\theta_0^{opt}$.

For all computations, the CARAMBA I configuration was assumed to be that of the rings in the cylindrical array. Thus the radius = 13.2 wavelengths, and 128 elements were assumed equally spaced on each ring, with 32 elements active. The amplitude distribution $I^c(\alpha_p)$ is one computed for the lens using a 1-3-3-1 input distribution. It is shown below with the 32-element Taylor distribution assumed for the distribution $I^e(Z_q)$. The spacing of the rings was 0.524 wavelength.

| Element or Ring Number | $I^e(Z_q)$ | $I^c(\alpha_p)$ |
|---|---|---|
| 1 | 1.000 | .9964 |
| 2 | .990 | .9682 |
| 3 | .970 | .9139 |
| 4 | .935 | .8373 |
| 5 | .885 | .7439 |
| 6 | .822 | .6397 |
| 7 | .755 | .5316 |
| 8 | .676 | .4258 |
| 9 | .597 | .3278 |
| 10 | .513 | .2419 |
| 11 | .437 | .1708 |
| 12 | .351 | .1154 |
| 13 | .288 | .0752 |
| 14 | .233 | .0479 |
| 15 | .200 | .0303 |
| 16 | .192 | .0185 |

For the element pattern $G(\varphi - \alpha_p, \theta)$, an approximation to measured patterns was chosen. Including the phase due the location on the ring, it is

$$G(\varphi - \alpha_p, \theta) = \cos\theta \exp\left[1.9 \cos\theta \cos(\varphi - \alpha) + j2\pi\rho \cos\theta \cos(\theta - \alpha)\right]$$

Note that this expression gives (apart from the $\cos\theta$ outside of the exponential) an omnidirectional pattern at $\theta = 90$ degrees, as must be the case.

## CONCLUSIONS

As a result of the investigation of the possible use of linear-array techniques to implement a circularly symmetric cylindrical array for wideband use, some general conclusions can be drawn. Components developed for the linear array can provide the necessary bandwidth and can be combined with circular-array techniques to form pencil beams. If beam-pointing angles are to be independent of frequency, then time-delay techniques can be used for elevation-beam steering. However, a digital-phase system of the CARAMBA II type provides a highly versatile tool for investigating the effects of amplitude and phase errors on the pencil-beam shape, side-lobe level, and beam-pointing angle in the elevation plane. Computer results indicate that optimization of the excitation distribution for a given elevation angle can extend the sector in the elevation plane over which the azimuth-beam maintains a useful shape. The implementation of this type of cylindrical array appears feasible.

## RECOMMENDATIONS

1. Investigate the implementation of a sector of a cylindrical array to produce a pencil beam.

2. Verify experimental computer predictions of optimum excitation distributions, and of elevation-scanning limitations and approximations.

3. Investigate techniques to provide multi-aperture, multifrequency capability to the cylindrical array.

# REFERENCES


1. Naval Electronics Laboratory Center Report 1501, *Circular-Array Radar Antenna,* by J. H. Provencher and B. I. Small, 7 July 1967

2. Naval Electronics Laboratory Center Report 1521, *Current Distributions and Radiation Patterns for Circular-Array Radar Antenna: Theory,* by A. D. Munger, 26 October 1967

3. Naval Electronics Laboratory Center Report 1535, *Circular-Array Radar Antenna: CARAMBA I Experimental Results,* by J. E. Boyns, 2 February 1968

4. Butler, J. and Lowe, R., "Beam-Forming Matrix Simplifies Design of Electronically Scanned Antennas," *Electronic Design,* v. 9, p. 170-173, 12 April 1961

5. Navy Electronics Laboratory Report 1468, *The Multithrow Microwave Diode Switch,* by J. Reindel, 16 June 1967

6. Boyns, J. E. and others, "A Lens Feed for a Ring Array," *Institute of Electrical and Electronic Engineers. Transactions: Antennas and Propagation,* v. AP-16, p. 91-92A, March 1968

7. Naval Electronics Laboratory Center Report 1522, *Beamwidths and Current Distributions for Circular-Array Antennas: Tables,* by A. D. Munger and J. H. Provencher, 26 October 1967

UNCLASSIFIED
Security Classification

**DOCUMENT CONTROL DATA - R & D**

*(Security classification of title, body of abstract and indexing annotation must be entered when the overall report is classified)*

1 ORIGINATING ACTIVITY *(Corporate author)*
NAVAL ELECTRONICS LABORATORY CENTER
for Command Control and Communications
San Diego, California 92152

2a. REPORT SECURITY CLASSIFICATION
UNCLASSIFIED

2b. GROUP

3. REPORT TITLE
CIRCULAR-ARRAY RADAR ANTENNA: PENCIL-BEAM FORMING AND PHASING TECHNIQUES

4 DESCRIPTIVE NOTES *(Type of report and inclusive dates)*
Research and Development Report, September 1967 - January 1968

5 AUTHOR(S) *(First name, middle initial, last name)*
J. H. Provencher and A. D. Munger

| 6. REPORT DATE | 7a. TOTAL NO. OF PAGES | 7b. NO OF REFS |
|---|---|---|
| 12 March 1968 | 58 | 7 |

| 8a. CONTRACT OR GRANT NO. | 9a. ORIGINATOR'S REPORT NUMBER(S) |
|---|---|
| b. PROJECT NO. SF 001 02 05<br>Task 6072<br>c. (NELC D11571)<br>d. | 1543 |
| | 9b. OTHER REPORT NO(S) *(Any other numbers that may be assigned this report)* |

10. DISTRIBUTION STATEMENT Each transmittal of this document outside the agencies of the U.S. Government must have prior approval of the Naval Electronics Laboratory Center for Command Control and Communications, San Diego, California 92152

| 11. SUPPLEMENTARY NOTES | 12. SPONSORING MILITARY ACTIVITY |
|---|---|
| | Naval Ship Systems Command<br>Department of the Navy |

13 ABSTRACT

Several linear and ring-array beam-forming techniques were examined to determine how they might contribute to achieving pencil-beam antennas from cylindrical configurations. Techniques adapted from the SAMB (Stationary Aperture Moving Beam) and CARAMBA (Circular-Array Radar Agile Moving Beam Antenna) programs are useful in advancing the basic cylindrical-array concept. Preliminary computer predictions indicate that a combination of the lens-feed technique and a linear array as an element of a ring array is a possible method of enabling a cylindrical array to produce a pencil beam.

DD FORM 1 NOV 65 1473 (PAGE 1)
S/N 0101-807-6801

UNCLASSIFIED
Security Classification

| 14 KEY WORDS | LINK A | | LINK B | | LINK C | |
|---|---|---|---|---|---|---|
| | ROLE | WT | ROLE | WT | ROLE | WT |
| Antenna arrays | | | | | | |
| Radar antennas | | | | | | |
| CARAMBA | | | | | | |

# INITIAL DISTRIBUTION LIST

CHIEF OF NAVAL MATERIAL
MAT 0331
COMMANDER, NAVAL SHIP SYSTEMS COMMAND
SHIPS 035
SHIPS 03522
SHIPS 2052 (2)
SHIPS 204113
COMMANDER, NAVAL AIR SYSTEMS COMMAND
AIR 5104
AIR 5330
AIR 5336
AIR 604
COMMANDER, NAVAL ORDNANCE SYSTEMS COMMAND
ORD 03C
ORD 0322
ORD 083
ORD 9132
COMMANDER, NAVAL ELECTRONIC SYSTEMS COMMAND
ELEX 913
COMMANDER, NAVAL SHIP ENGINEERING CENTER
CODE 6170
CODE 6175B
CODE 6175.02
CODE 6176
CODE 6178
CODE 61790
CODE 6179C07
NAVAL SHIP ENGINEERING CENTER
SAN DIEGO DIVISION
CHIEF OF NAVAL PERSONNEL
PERS 11B
CHIEF OF NAVAL OPERATIONS
OP-03EG
OP-345
OP-506G
OP-07T
OP-724
OP-0985
OP-922F4C1
OP-94G
CHIEF OF NAVAL RESEARCH
CODE 418
CODE 427
CODE 455
CODE 461
COMMANDER IN CHIEF
US PACIFIC FLEET
CODE 93
US ATLANTIC FLEET
COMMANDER OPERATIONAL TEST AND EVALUATION FORCE
DEPUTY COMMANDER OPERATIONAL TEST AND EVALUATION FORCE, PACIFIC
COMMANDER CRUISER-DESTROYER FORCE
US PACIFIC FLEET
CODE 425
US ATLANTIC FLEET
COMMANDER SUBMARINE FORCE
US PACIFIC FLEET
COMMANDER ANTISUBMARINE WARFARE FORCE
US PACIFIC FLEET
US ATLANTIC FLEET
COMMANDER FIRST FLEET
COMMANDER SECOND FLEET
COMMANDER TRAINING COMMAND
US PACIFIC FLEET
US ATLANTIC FLEET
COMMANDER AMPHIBIOUS FORCE, US PACIFIC FLEET
COMMANDER SERVICE FORCE, US ATLANTIC FLEET
COMMANDER, DESTROYER DEVELOPMENT GROUP, PACIFIC
COMMANDER FLEET AIR WINGS, ATLANTIC FLEET
NAVAL AIR DEVELOPMENT CENTER
LIBRARY
NAVAL MISSILE CENTER
TECHNICAL LIBRARY
CODE N3232
PACIFIC MISSILE RANGE
CODE 3250
NAVAL AIR TEST CENTER
NANEP
WEAPONS SYSTEMS TEST DIVISION
NAVAL WEAPONS CENTER
CHINA LAKE
CODE 753
CORONA LABORATORIES
TECHNICAL LIBRARY
NAVAL UNDERSEA WARFARE CENTER
LIBRARY
FLEET COMPUTER PROGRAMMING CENTER
PACIFIC
LIBRARY
ATLANTIC
TECHNICAL LIBRARY
NAVAL WEAPONS LABORATORY
LIBRARY
PEARL HARBOR NAVAL SHIPYARD
CODE 246P
PORTSMOUTH NAVAL SHIPYARD
CODE 242L
SAN FRANCISCO BAY NAVAL SHIPYARD
PHILADELPHIA NAVAL SHIPYARD
CODE 249C
CHARLESTON NAVAL SHIPYARD
CODE 240
NAVAL SHIP RESEARCH & DEVELOPMENT CENTER
CARDEROCK DIVISION
LIBRARY
NAVY MINE DEFENSE LABORATORY
CODE 716
NAVAL TRAINING DEVICE CENTER
TECHNICAL LIBRARY
NAVY UNDERWATER SOUND LABORATORY
LIBRARY
NAVAL AIR ENGINEERING CENTER
AEROSPACE CREW EQUIPMENT LABORATORY
LIFE SCIENCES RESEARCH GROUP
NAVAL CIVIL ENGINEERING LABORATORY
L54
NAVAL RESEARCH LABORATORY
CODE 2027
CODE 5250
CODE 5320
CODE 5330
CODE 5400
CODE 5440
NAVAL ORDNANCE LABORATORY, WHITE OAK
DIVISION 730
BEACH JUMPER UNIT ONE
BEACH JUMPER UNIT TWO
FLEET ASW SCHOOL
TACTICAL LIBRARY
NAVAL UNDERWATER WEAPONS RESEARCH AND ENGINEERING STATION
LIBRARY
OFFICE OF NAVAL RESEARCH BRANCH OFFICE
PASADENA
CHIEF SCIENTIST
BOSTON
CHICAGO
LONDON
NAVAL SHIP MISSILE SYSTEMS ENGINEERING STATION
CODE 903
NAVAL AIR TECHNICAL TRAINING CENTER
85
NAVAL PERSONNEL RESEARCH ACTIVITY
SAN DIEGO
WEATHER RESEARCH FACILITY
NAVAL OCEANOGRAPHIC OFFICE
CODE 1640
SUPERVISOR OF SHIPBUILDING, CONVERSION & REPAIR, US NAVY
GROTON, CONN.
CODE 249
NAVAL POSTGRADUATE SCHOOL
DEPT. OF ENVIRONMENTAL SCIENCES
LIBRARY
NAVAL APPLIED SCIENCE LABORATORY
CODE 222
CODE 920
NAVAL ACADEMY
ASSISTANT SECRETARY OF THE NAVY (RESEARCH AND DEVELOPMENT)
NAVAL SCIENTIFIC AND TECHNICAL INTELLIGENCE CENTER (IE)
NAVAL SECURITY GROUP
G43
COMMANDANT OF THE MARINE CORPS
OFFICE OF THE DEPUTY CHIEF OF STAFF RESEARCH AND DEVELOPMENT
G-2
CODE A02D
AIR DEVELOPMENT SQUADRON ONE
VX-1
DEFENSE DOCUMENTATION CENTER (20)
DEPARTMENT OF DEFENSE RESEARCH AND ENGINEERING
TECHNICAL LIBRARY
WEAPONS SYSTEMS EVALUATION GROUP
FEDERAL AVIATION AGENCY
SYSTEMS RESEARCH AND DEVELOPMENT SERVICE
MILITARY COORDINATION (RD-52.1)
COAST GUARD HEADQUARTERS
OSR-2
COAST AND GEODETIC SURVEY
WASHINGTON, D. C.
FEDERAL COMMUNICATIONS COMMISSION
RESEARCH DIVISION
US WEATHER BUREAU
DIRECTOR, METEOROLOGICAL RESEARCH
NATIONAL SEVERE STORMS LABORATORY
CENTRAL INTELLIGENCE AGENCY
OCR/DD-STANDARD DIST.
NATIONAL SECURITY AGENCY
C-15
P-224
R-31
DEFENSE COMMUNICATIONS AGENCY
COMMUNICATIONS SATELLITE PROJECT OFFICE
NATIONAL BUREAU OF STANDARDS
BOULDER, COLO.
BUREAU OF COMMERCIAL FISHERIES
LA JOLLA, CALIF.
FISHERY-OCEANOGRAPHY CENTER LIBRARY
TUNA RESOURCES LABORATORY LA JOLLA
WOODS HOLE, MASS.
BIOLOGICAL LABORATORY LIBRARY
ELECTROMAGNETIC COMPATIBILITY ANALYSIS CENTER
NAVENGRXSTA
NAFEC LIBRARY
ARMY MATERIAL COMMAND
AMCRD-DE-E-S
ASST CHIEF OF STAFF FOR INTELLIGENCE, US ARMY
SYSTEMS DEVELOPMENT DIVISION
ABERDEEN PROVING GROUND
TECHNICAL LIBRARY
ARMY TEST AND EVALUATION COMMAND
MDOTRS AMSTE-EL
ARMY RESEARCH AND DEVELOPMENT ACTIVITY
ELECTRONIC WARFARE DIVISION
ELECTRONIC DEPARTMENT
ARMY MISSILE COMMAND
REDSTONE SCIENTIFIC INFORMATION CENTER
DOCUMENT SECTION
ARMY ELECTRONICS RESEARCH AND DEVELOPMENT LABORATORY
ARMY ELECTRONICS COMMAND
ELECTRONIC WARFARE LABORATORY
AMSEL-WL-D
MANAGEMENT & ADMINISTRATIVE SERVICES DEPT
AMSEL-RD-MAT
COMBAT SURVEILLANCE & TARGET ACQUISITION
AMSEL-RL-R
INSTITUTE FOR EXPLORATORY RESEARCH
AMSEL-XL-C
HARRY DIAMOND LABORATORIES
LIBRARY
FRANKFORD ARSENAL
HUMAN FACTORS LABORATORY
SMUFA N6400/202-4
PICATINNY ARSENAL
TECHNICAL INFORMATION BRANCH
SMUPA-VA6
ARMY RESEARCH OFFICE (DURHAM)
CRD-AA-IP
WHITE SANDS MISSILE RANGE
STEWS-IO-E
HUMRRO DIVISION NO. 2 (ARMOR)
LIBRARIAN
ARMY ELECTRONIC WARFARE LABORATORY
MOUNTAIN VIEW OFFICE
ARMY AIR DEFENSE BOARD
SUPPORT DIVISION
FORT HUACHUCA
52D USASASOC
ARMY ENGINEER RESEARCH AND DEVELOPMENT LABORATORIES
TECHNICAL DOCUMENT CENTER
AIR FORCE HEADQUARTERS
DIRECTOR OF COMMAND CONTROL & COMMUNICATIONS
AFOCCBC
AIR DEFENSE COMMAND
ADOOA
AIR UNIVERSITY LIBRARY
AUL/IT-5028
STRATEGIC AIR COMMAND
DAST
AIR FORCE EASTERN TEST RANGE
AFMTC TECHNICAL LIBRARY - MU-135
ROME AIR DEVELOPMENT CENTER
EMLAL-1 (DOCUMENT LIBRARY)
EMIA
AIR PROVING GROUND CENTER
PGBPS-12
1ST STRATEGIC AEROSPACE DIVISION
OCI
HEADQUARTERS AIR WEATHER SERVICE
AWSSS/SIPD
WRIGHT-PATTERSON AIR FORCE BASE
AVWE-3, ANTENNA-RADOME GROUP
SEG/SEODE
AIR FORCE SECURITY SERVICE
ESD/ESG
ELECTRONICS SYSTEMS DIVISION
ESTI
UNIVERSITY OF MICHIGAN
OFFICE OF RESEARCH ADMINISTRATION
NORTH CAMPUS
EDITORIAL OFFICE
COOLEY ELECTRONICS LABORATORY
RADAR AND OPTICS LABORATORY
THE RADIATION LABORATORY
UNIVERSITY OF CALIFORNIA-BERKELEY
ELECTRONICS RESEARCH LABORATORY
UNIVERSITY OF CALIFORNIA-LOS ANGELES
ENGINEERING DEPARTMENT
MICHIGAN STATE UNIVERSITY
LIBRARY-DOCUMENTS DEPARTMENT
INSTITUTE OF COURANT
MATHEMATICAL SCIENCES
COLUMBIA UNIVERSITY
ELECTRONIC RESEARCH LABORATORIES
DARTMOUTH COLLEGE
RADIOPHYSICS LABORATORY
CALIFORNIA INSTITUTE OF TECHNOLOGY
JET PROPULSION LABORATORY
UNIVERSITY OF ILLINOIS
DEPARTMENT OF PSYCHOLOGY
ELECTRICAL ENGINEERING DEPARTMENT
CORNELL UNIVERSITY
LIBRARY, CENTER FOR RADIOPHYSICS AND SPACE RESEARCH
HARVARD COLLEGE OBSERVATORY
HARVARD UNIVERSITY
GORDON MCKAY LIBRARY
LYMAN LABORATORY
GEORGIA INSTITUTE OF TECHNOLOGY
ENGINEERING EXPERIMENT STATION
ELECTRONICS DIVISION
UNIVERSITY OF WASHINGTON
APPLIED PHYSICS LABORATORY
TUFTS UNIVERSITY
INSTITUTE FOR PSYCHOLOGICAL RESEARCH
OHIO STATE UNIVERSITY
ANTENNA LABORATORY
UNIVERSITY OF ALASKA
GEOPHYSICAL INSTITUTE
UNIVERSITY OF HAWAII
ELECTRICAL ENGINEERING DEPARTMENT
THE UNIVERSITY OF TEXAS
DEFENSE RESEARCH LABORATORY
STANFORD UNIVERSITY
STANFORD ELECTRONICS LABORATORIES
DOCUMENTS LIBRARY
STANFORD RESEARCH INSTITUTE
NAVAL WARFARE RESEARCH CENTER
MASSACHUSETTS INSTITUTE OF TECHNOLOGY
RESEARCH LABORATORY OF TECHNOLOGY
DOCUMENT ROOM
ENGINEERING LIBRARY
LINCOLN LABORATORY
LIBRARY, A-082
RADIO PHYSICS DIVISION
RADAR DIVISION
UNIVERSITY OF NEW MEXICO
BUREAU OF ENGINEERING RESEARCH
THE JOHNS HOPKINS UNIVERSITY
APPLIED PHYSICS LABORATORY
DOCUMENT LIBRARY
INSTITUTE FOR DEFENSE ANALYSES
DOCUMENT LIBRARY